

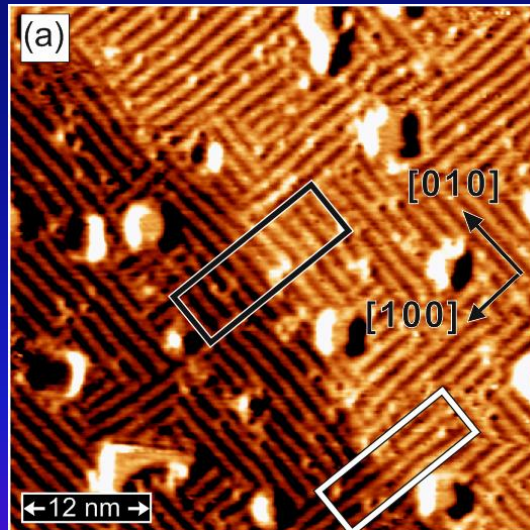
Quantum World at Atomic Scale: Spin-Polarized Scanning Tunneling Microscopy

Pin-Jui Hsu^{1,2} (徐斌睿)

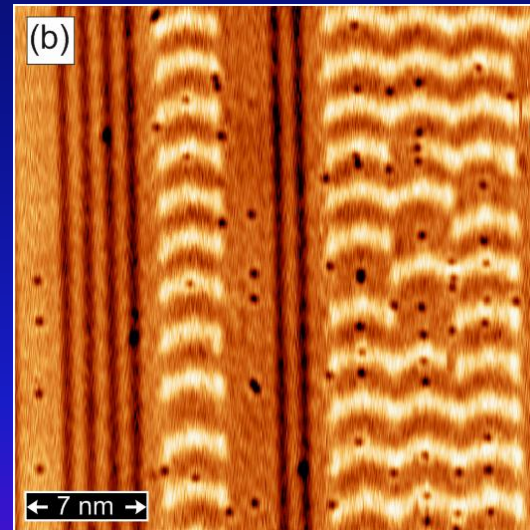
1. Institute of Applied Physics, University of Hamburg, Jungiusstrasse 11, D-20355 Hamburg, Germany

2. Department of Physics, National Tsing Hua University, No. 101, Section 2, Kuang-Fu Road, Hsinchu 30013, Taiwan

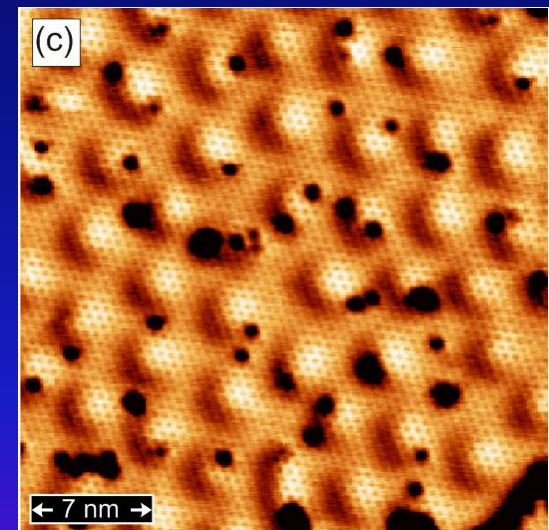
Fe-DL/ Rh(001)

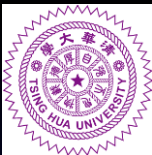


Fe-TL/ Ir(111)



H/ Fe-DL/ Ir(111)





Outline



➤ **Research Motivation**

- *To image, detect, and manipulate low-dimensional systems by SP-STM with spin resolution.*

➤ **Introductions & Literatures**

- *What SP-STM can do ?*

- ◆ *Atomic Spin Lattice : Non-collinear Magnetism*

- *Chiral Domain Wall, Spin Spiral, Magnetic Skyrmions*

- ◆ *SP-STS : LDOS, QPI, IETS, Image State, Landau Splitting, QPC*

- *Kondo Resonance, Band Dispersion, Phonon Excitation*

- ◆ *Atom Manipulation : Zeeman Splitting, Magnetic Hysteresis*

- *Magnetic Moment, Magnetocrystalline Anisotropy, RKKY Coupling Strength*

- ◆ *Time Resolution : Pump-Probe Dynamics, Atomic Dipolar Fields*

- *Electron Spin Resonance, Dipole-dipole Interaction*

➤ **Summary & Future Highlights**



Scanning Tunneling Microscopy

Background



The Nobel Prize in Physics 1986 ~

"See" the atomic scale world !!



Ernst Ruska

"for his fundamental work in electron optics, and for the design of the first electron microscope"



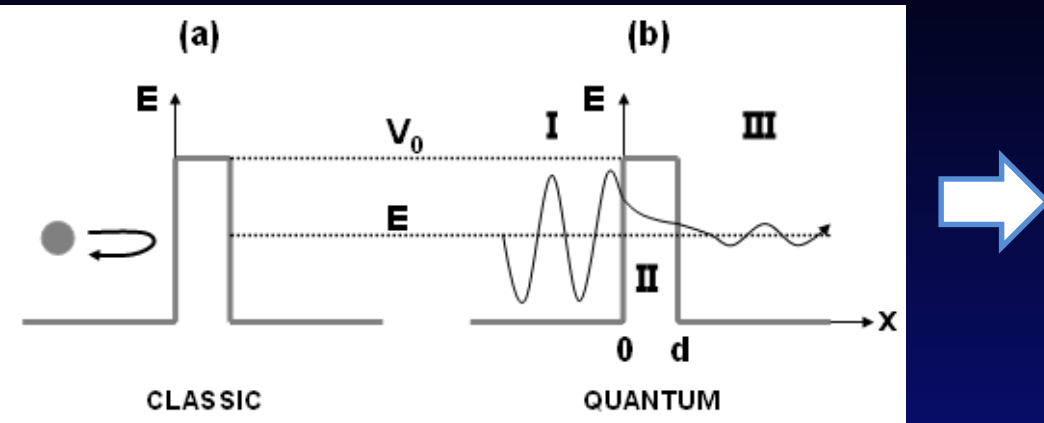
Gerd Binnig

Heinrich Rohrer

"for their design of the scanning tunneling microscope"

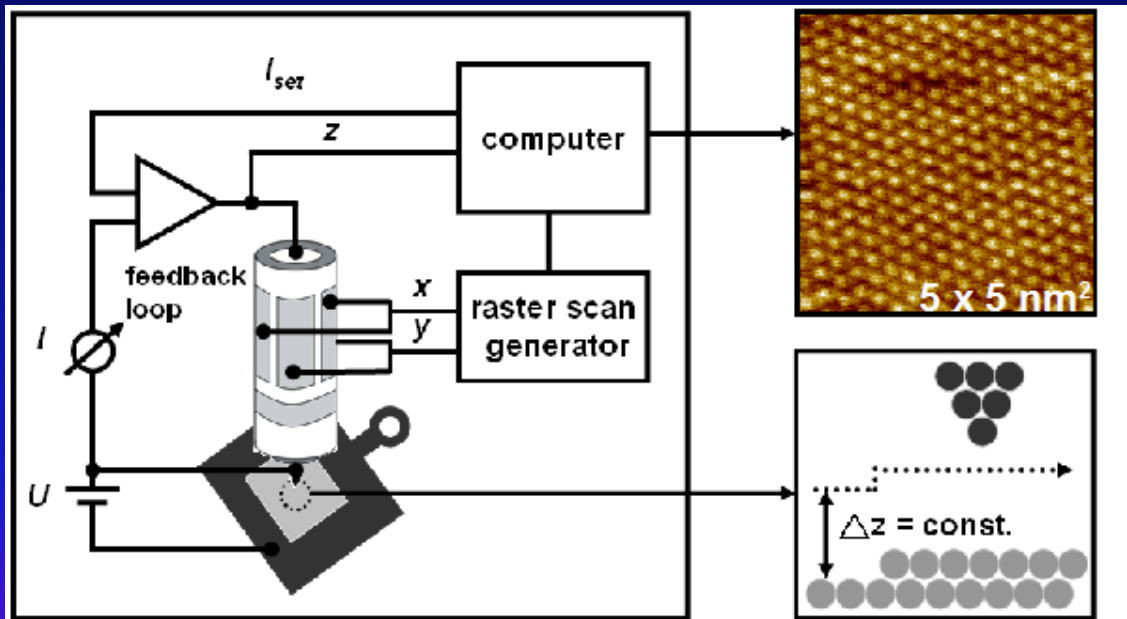
Scanning Tunneling Microscopy

Working Principle



$$T = \frac{j_t}{j_i} = \left| \frac{F}{A} \right|^2 = \frac{1}{1 + \frac{(k^2 + \kappa^2)^2}{(4k^2\kappa^2)} \sinh^2(\kappa d)}$$

$$T \approx \frac{16k^2\kappa^2}{(k^2 + \kappa^2)^2} \cdot e^{-2\kappa d}, \quad \kappa d \gg 1$$



$I \propto e^{-\lambda z}$

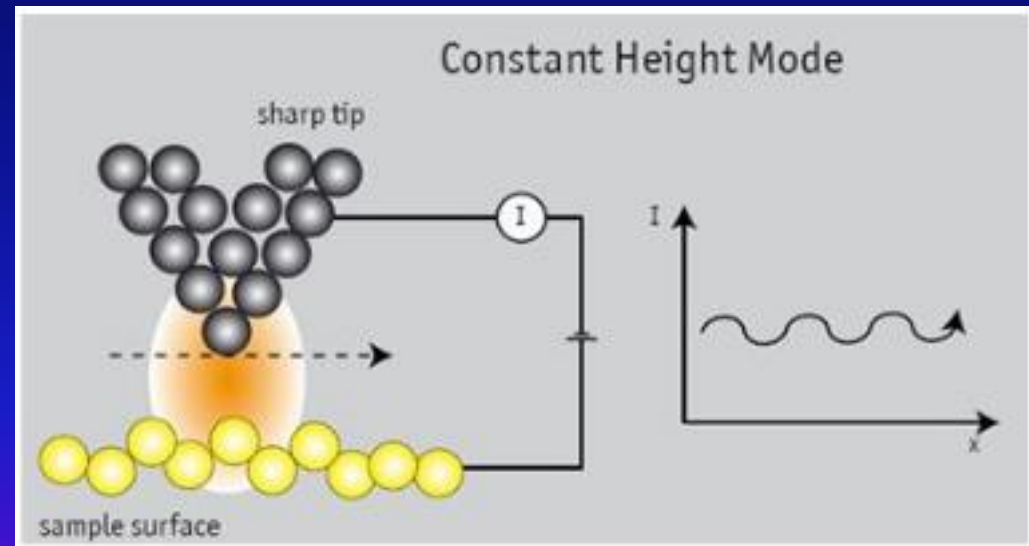
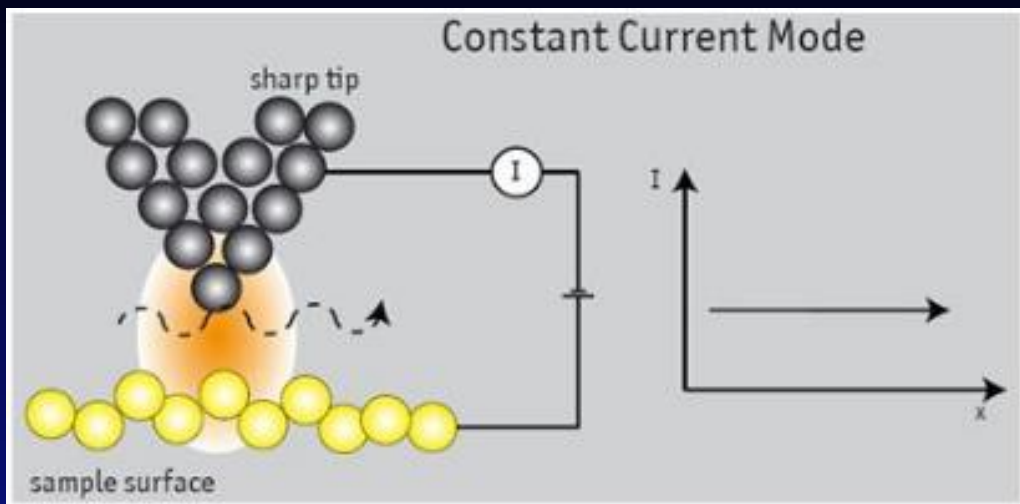
- Atomic Resolution
- Surface Sensitivity
- Local Density of States

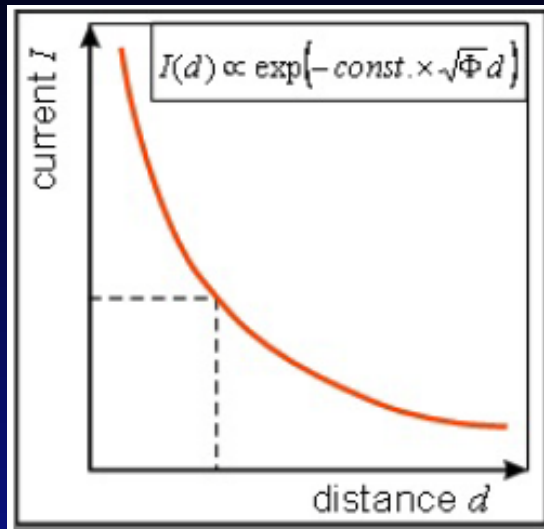
↓

(Tunneling Spectroscopy)

Scanning Tunneling Microscopy

Operation Modes





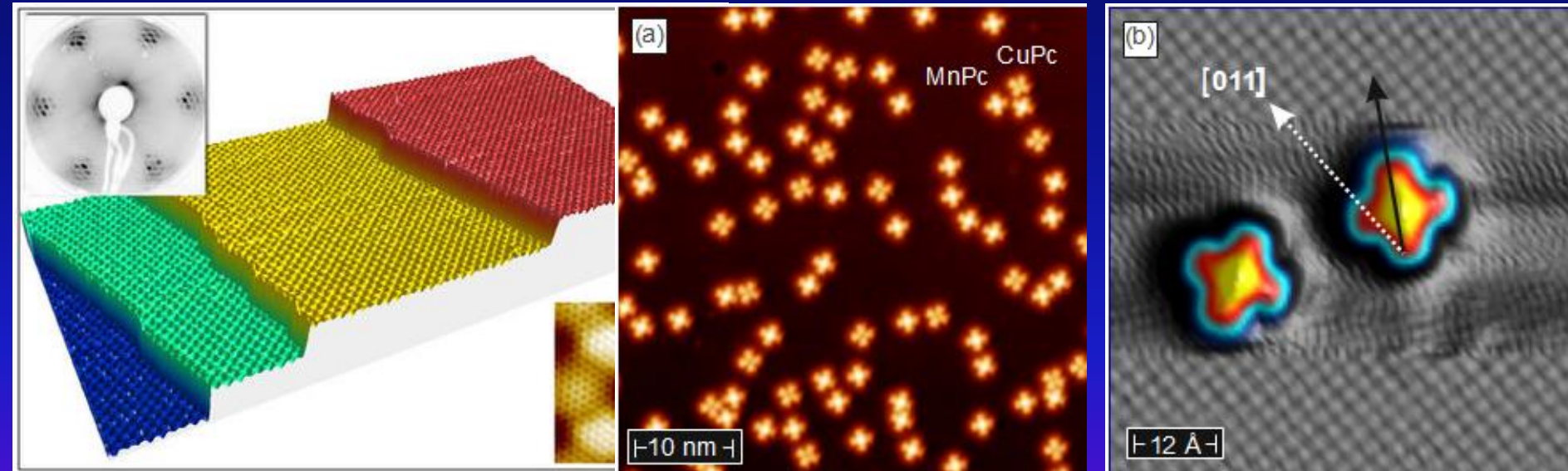
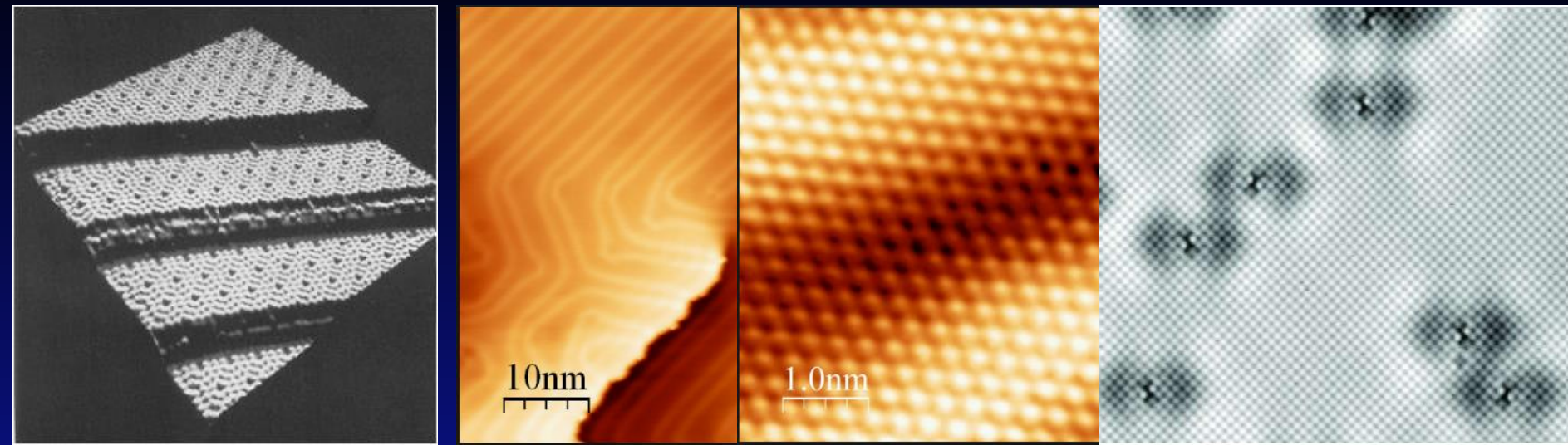
$$I(d) = \text{constant} \times eV \exp\left(-2 \frac{\sqrt{2m\Phi}}{\hbar} d\right)$$

Φ : the work function (energy barrier),
 e : the electron charge,
 m : the electron mass,
 h : the Planck's constant,
 V : applied voltage,
 d : tip-sample distance.

- A thin metal tip is brought in close proximity of the sample surface. At a distance of only a few Å, the overlap of tip and sample electron wavefunctions is large enough for an electron tunneling to occur.
- When an electrical voltage V is applied between sample and tip, this tunneling phenomenon results in a net electrical current, the 'tunneling current'. This current depends on the tip-surface distance d , on the voltage V , and on the height of the barrier Φ :
- This (approximate) equation shows that the tunneling current obeys Ohm's law, i.e. the current I is proportional to the voltage V .
- The current depends exponentially on the distance d .
- For a typical value of the work function Φ of 4 eV for a metal, the tunneling current reduces by a factor 10 for every 0.1 nm increase in d . This means that over a typical atomic diameter of e.g. 0.3 nm, the tunneling current changes by a factor 1000! This is what makes the STM so sensitive.
- The tunneling current depends so strongly on the distance that it is dominated by the contribution flowing between the last atom of the tip and the nearest atom in the specimen -- single-atom imaging!

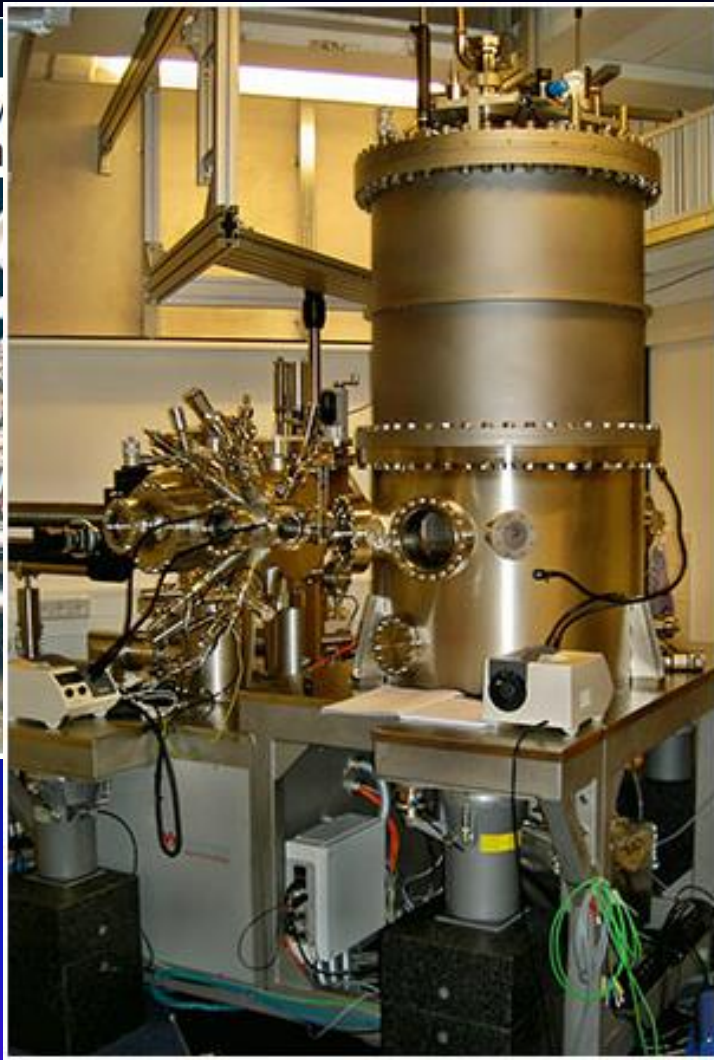
Scanning Tunneling Microscopy

Various Systems

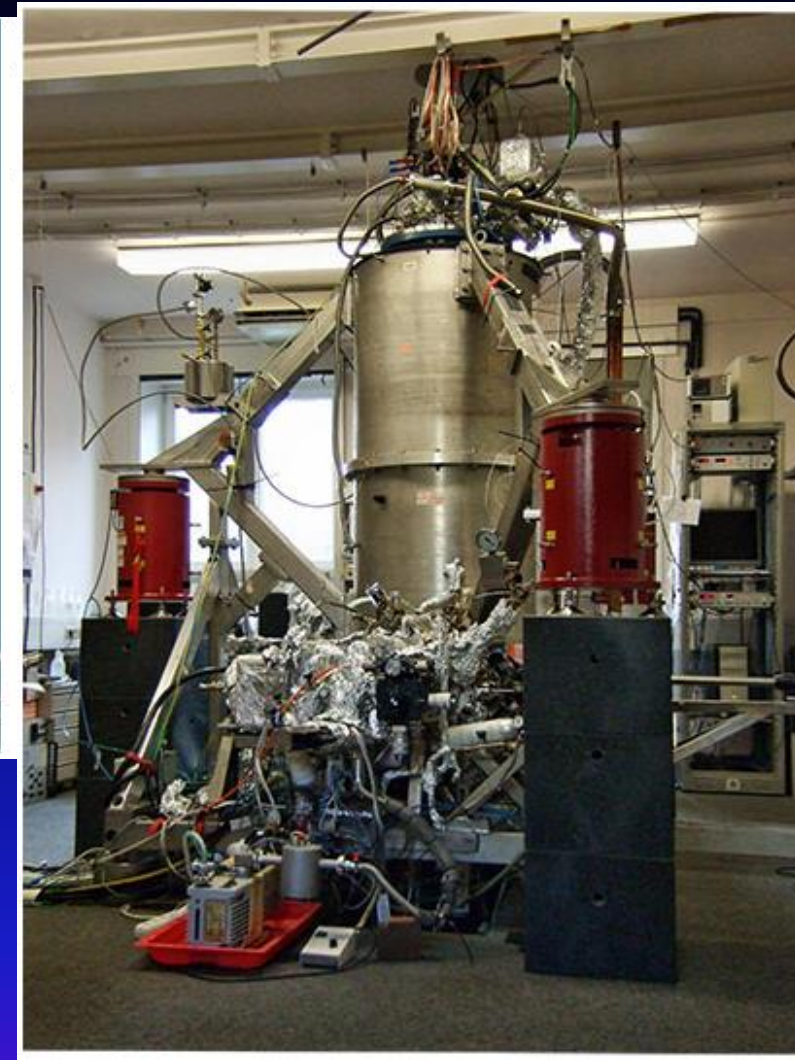


Experimental Instruments

Various types of STM in Hamburg



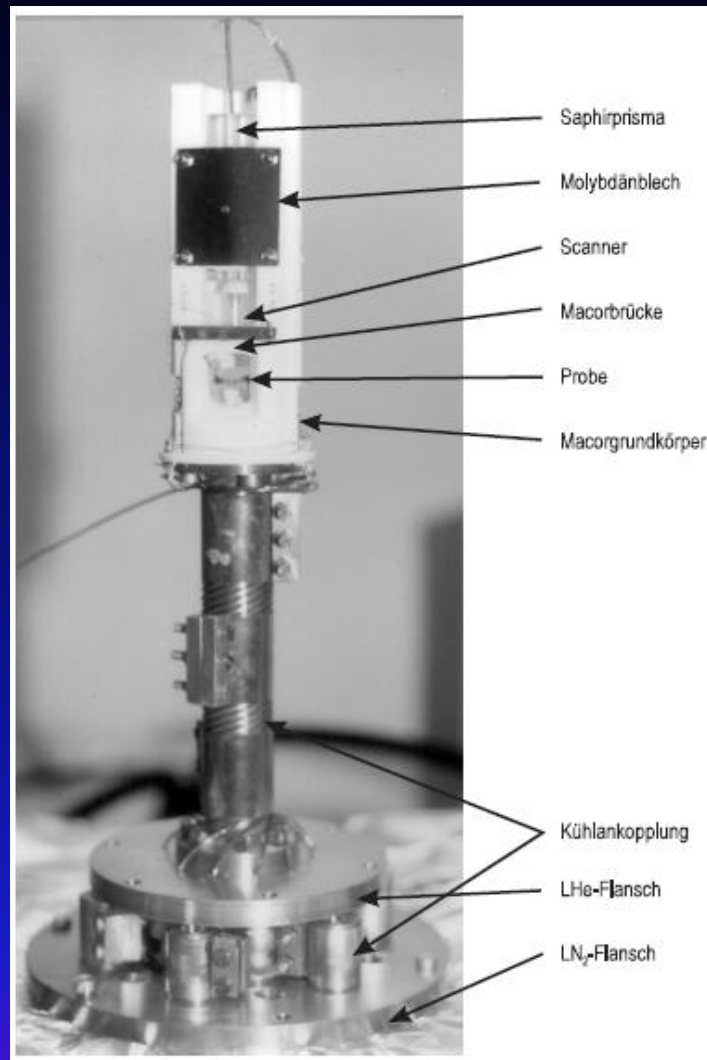
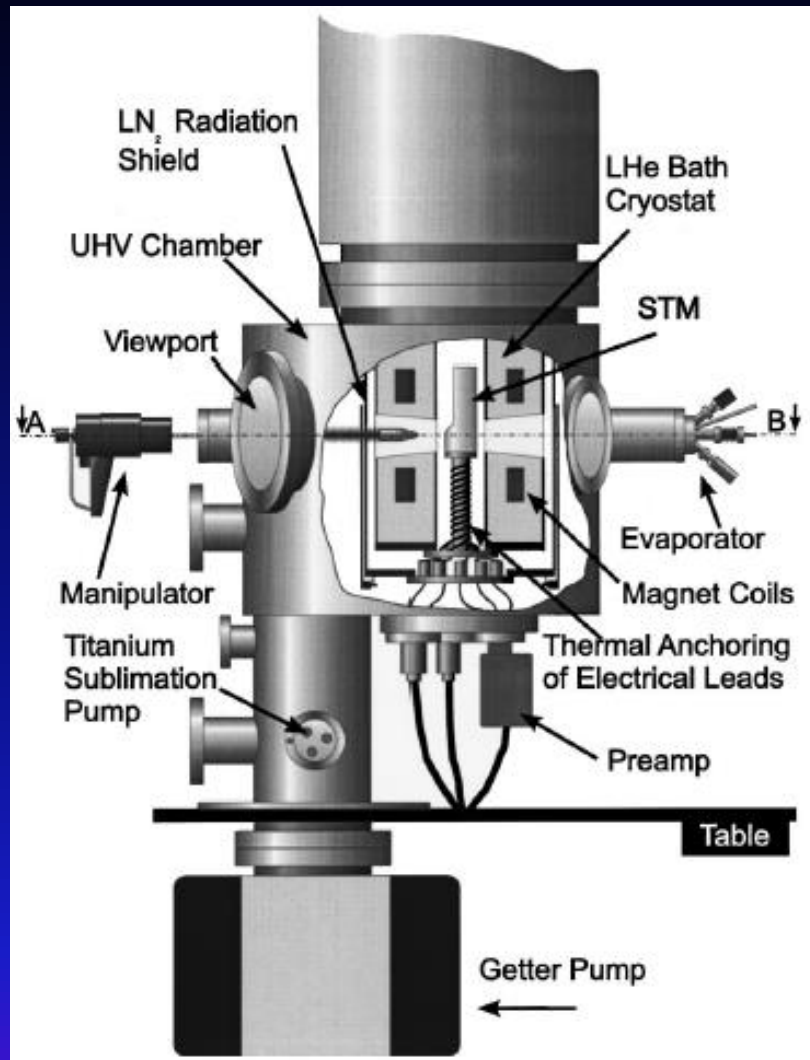
➤ Home built 4K-STM with 3D Magnets



➤ Home built 300 mK-STM with 12T Magnet

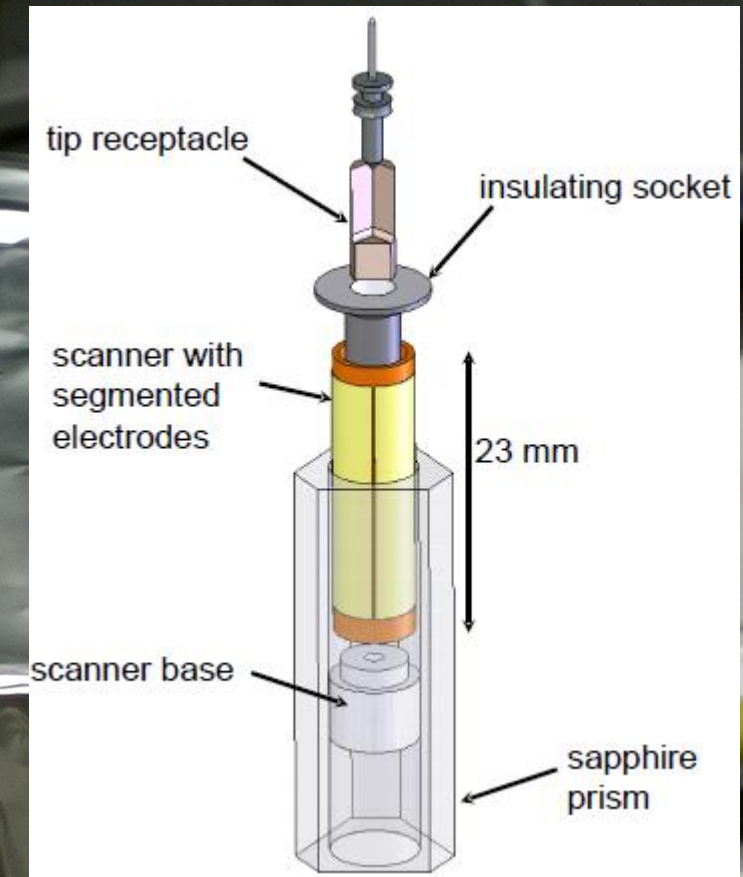
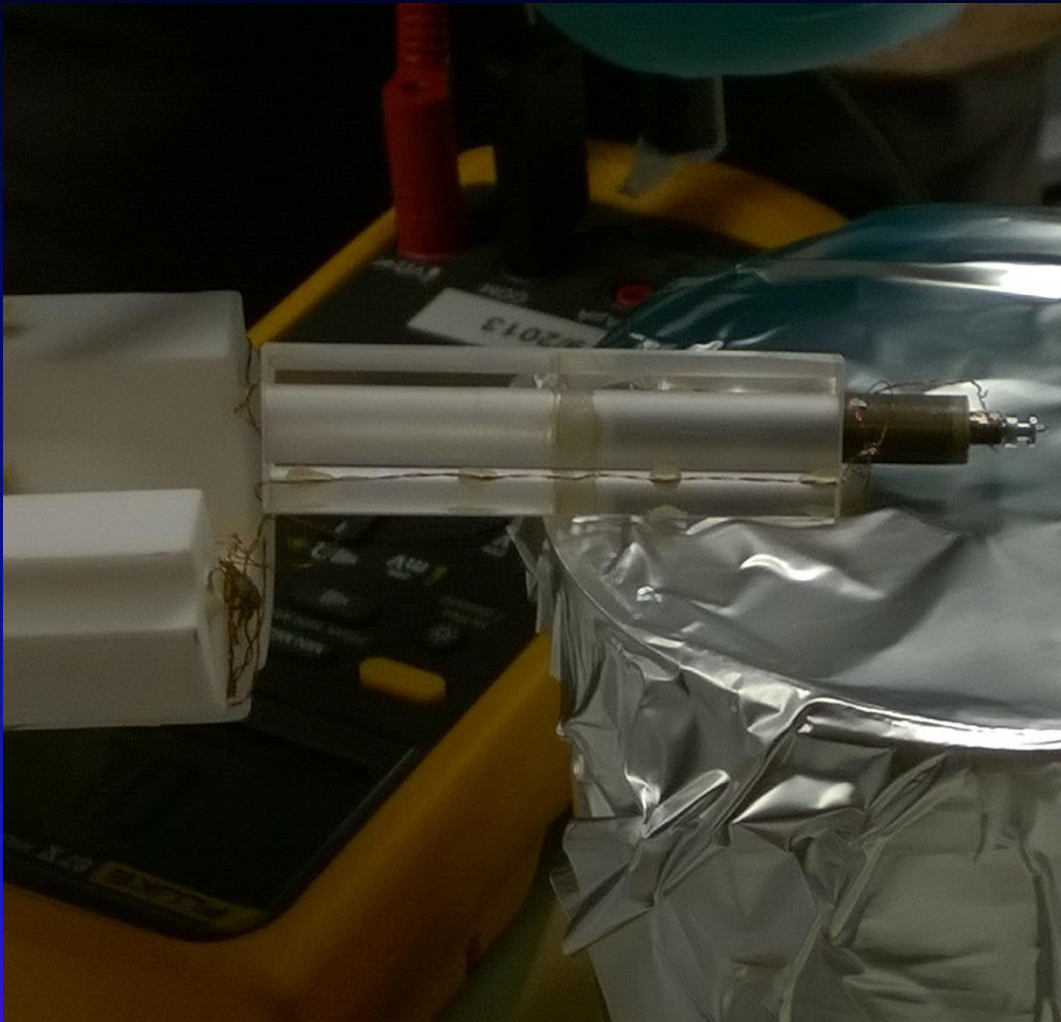
Experimental Instruments

Various types of STM in Hamburg



Experimental Instruments

Various types of STM in Hamburg

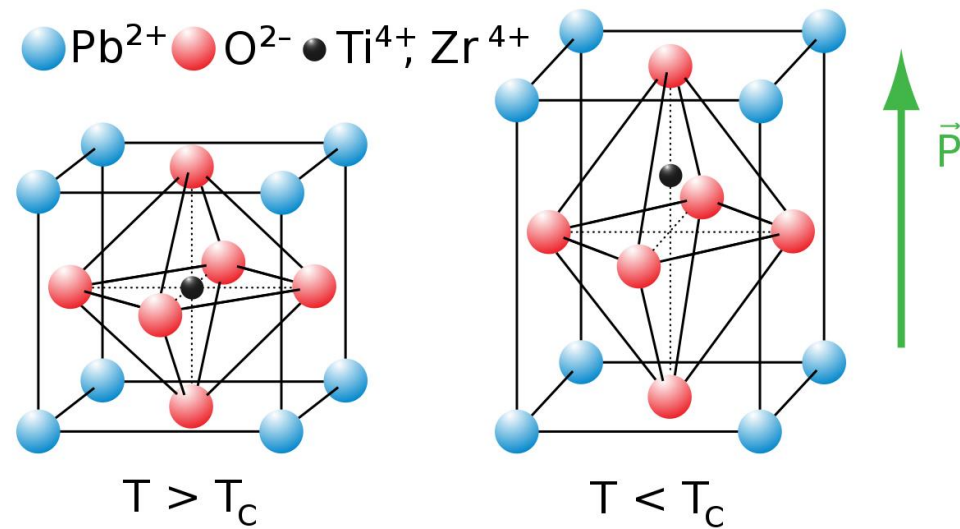
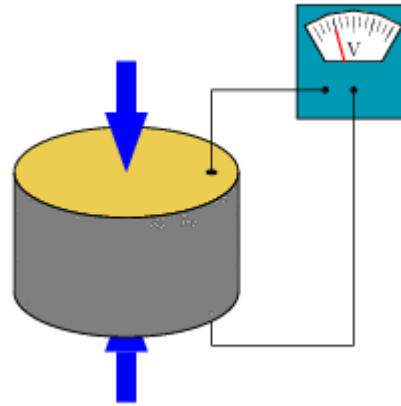


Scanning Tunneling Microscopy

Scanner Piezo Tube

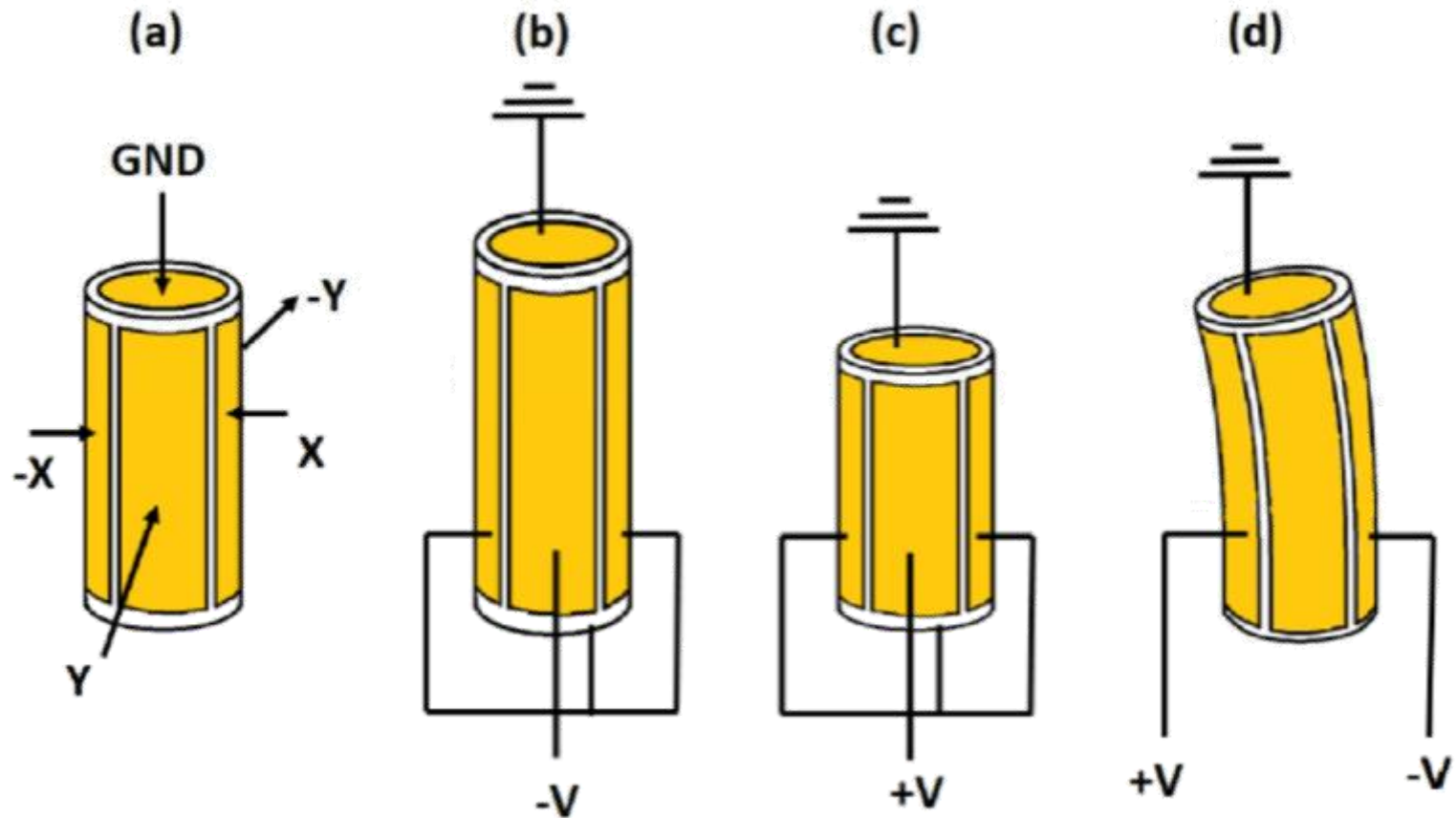


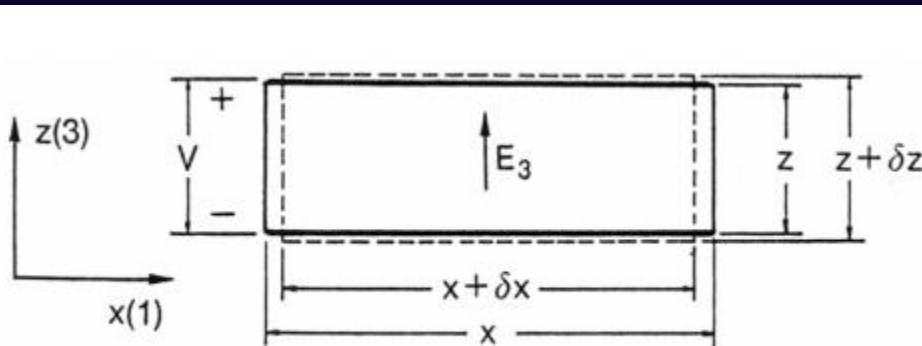
Tube Scanners



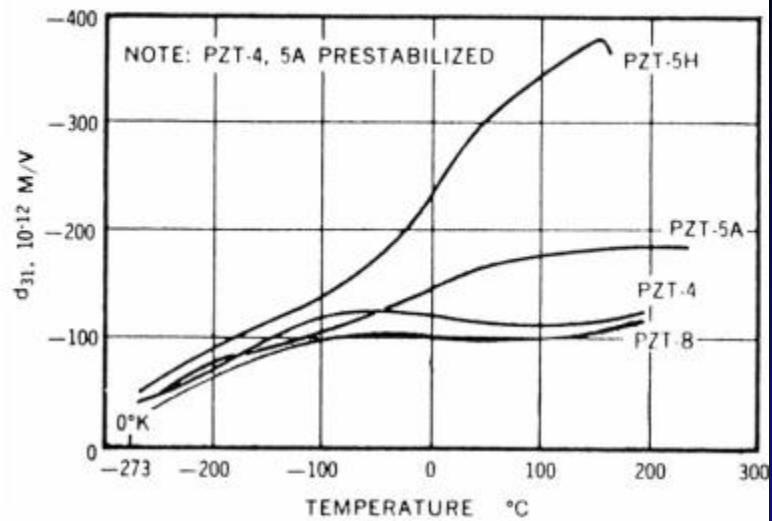
Scanning Tunneling Microscopy

Scanner Piezo Tube





Variation of piezoelectric coefficient with temperature.



Strain: $S_1 = \delta x/x$, $S_3 = \delta z/z$

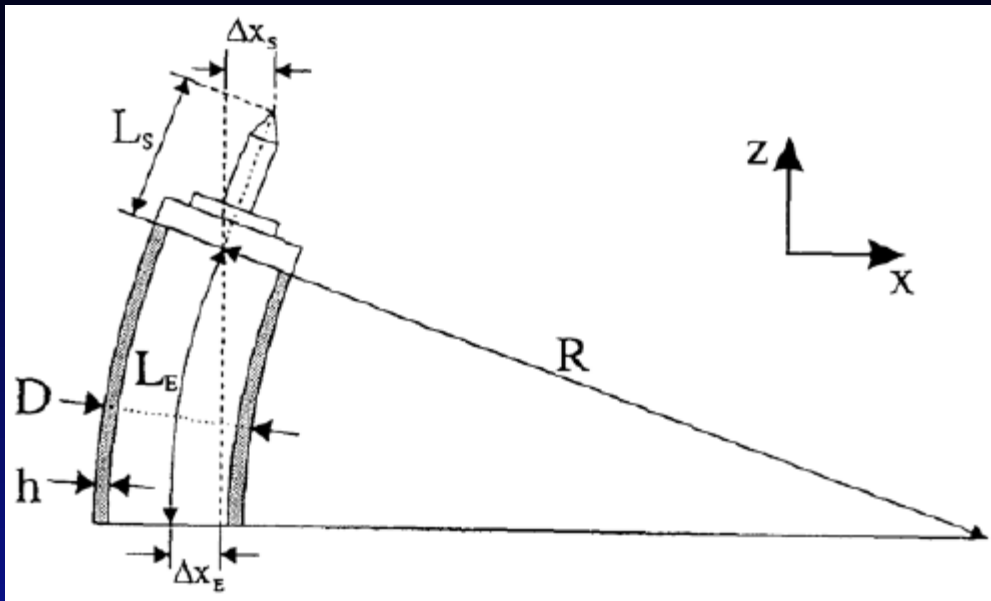
Electric field: $E_3 = V/z$

Piezoelectric Coeff.: $d_{33} = S_3/E_3$, $d_{31} = S_1/E_3$

Typical values for $d_{31} \sim -1 \text{ \AA/V}$, $d_{33} \sim 3 \text{ \AA/V}$.

Scanning Tunneling Microscopy

Scanner Piezo Tube



$$\Delta x = 2(\Delta x_E + \Delta x_S)$$

$$\Delta x = \Delta y = \frac{2\sqrt{2}d_{31}U}{\pi Dw}(L_E^2 + 2L_E L_S)$$

$$\Delta z = d_{31}U \frac{L_E}{w}$$

The scanner used has a wall thickness $w = 0.5$ mm and an outer diameter $D = 6.4$ mm. The length of the electrodes and the extension is $L_E = 19.5$ mm and $L_S = 8.6$ mm, respectively. The piezoelectric constant is $d_{31} = 9.5 \cdot 10^{-12}$ m/V and the maximal voltage which can be applied is $U = \pm 130$ V. The resulting scan range is:

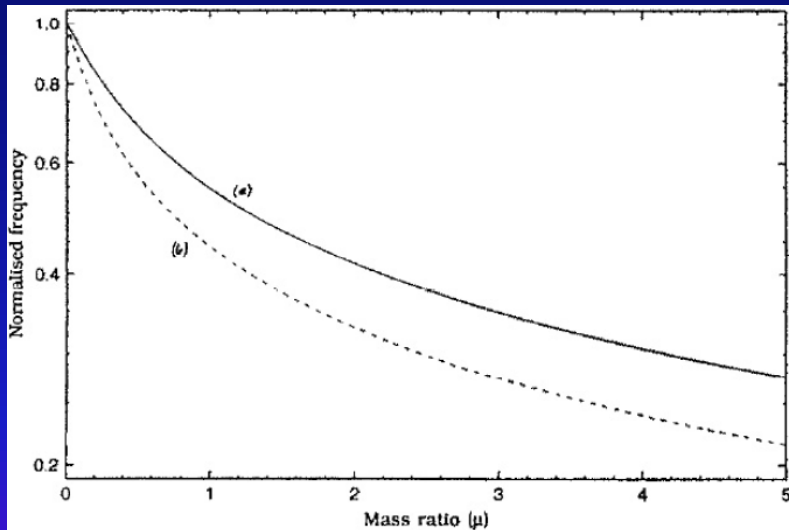
$$\begin{aligned}\Delta x = \Delta y &= 4.934 \mu\text{m} \\ \Delta z &= 0.948 \mu\text{m}\end{aligned}$$

The transverse and longitudinal eigenfrequencies – f_l and f_t – of the scanner have to be larger than the typical cut-off frequencies used in STM-experiments (about 1.5 kHz).

$$f_l = \frac{1}{4L} \sqrt{\frac{E}{\rho}} = 36.592 \text{ kHz}$$

$$f_t = \frac{1.88^2 D}{4\sqrt{2}\pi L^2} \sqrt{\frac{E}{\rho}} = 8.037 \text{ kHz}$$

$L = 23$ mm is the entire scanner length, $D = 6.4$ mm is the diameter of the tube. $E = 8.5 \cdot 10^{10}$ N/m² is Young's modulus and $\rho = 7500$ kg/m³ is the density of the tube's material.



The frequencies are lowered due to the load of the scanner. i.e. the entire mass of insulating socket, tip receptacle, tip holder and tip. Figure 3.8 shows that the mass ratio $\mu = 0, 5$, i.e. external load divided by the tube's mass, can be used to determine the normalized eigenfrequencies:

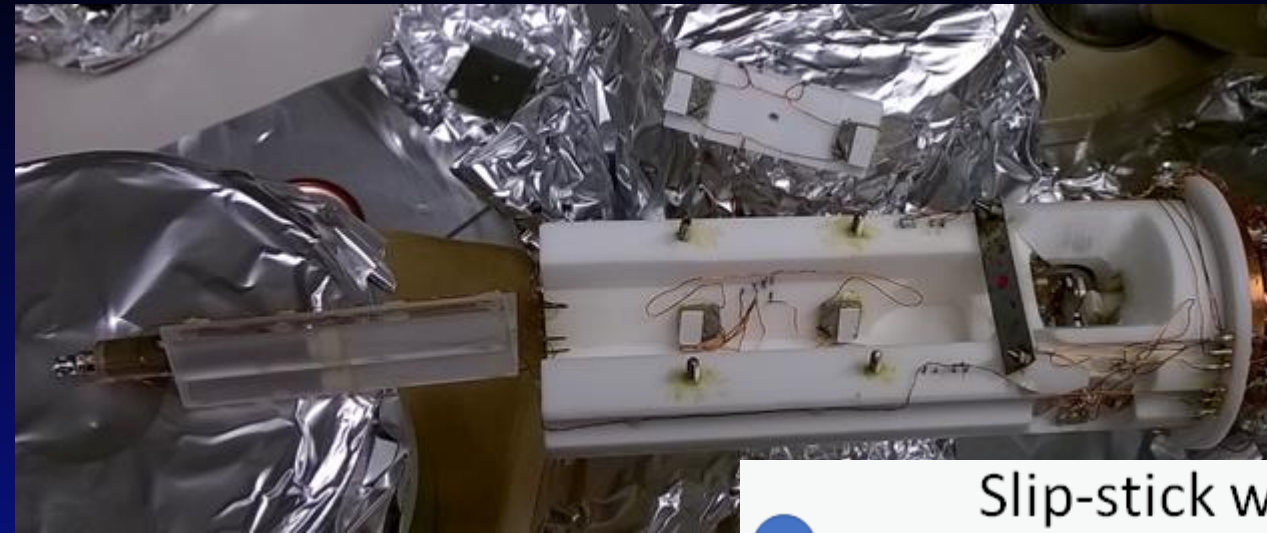
$$f_l = 18.296 \text{ kHz}$$

$$f_t = 4.661 \text{ kHz}$$

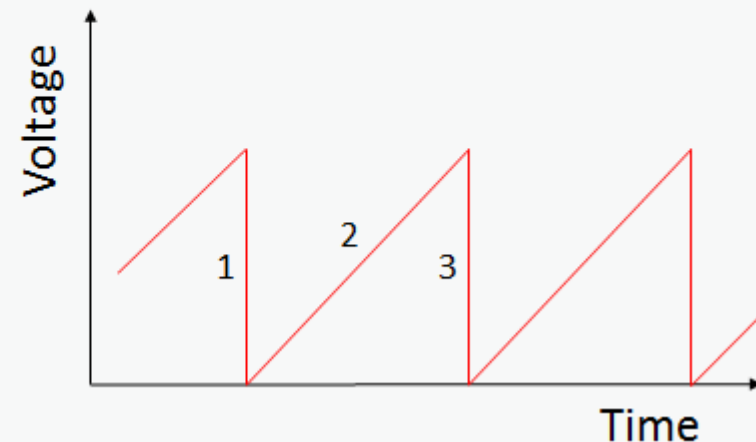
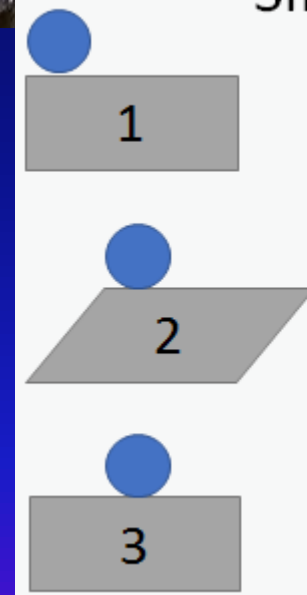
Dependence of the eigenfrequencies (extension (a), deflection (b))

Scanning Tunneling Microscopy

Coarse Piezo Motor

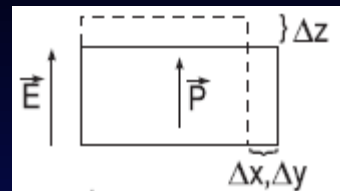
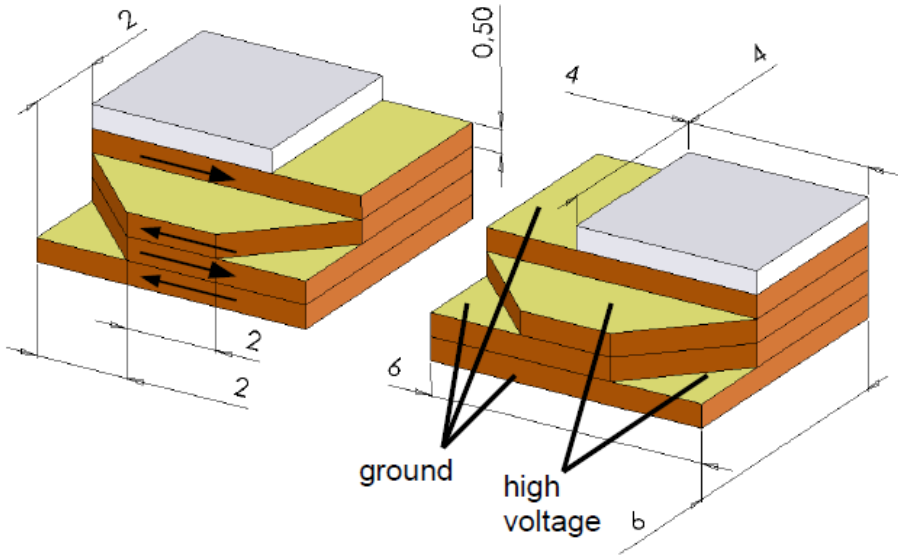


Slip-stick walking motion

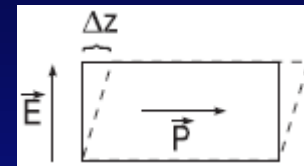


Scanning Tunneling Microscopy

Coarse Piezo Motor



Längs-Effekt: $\Delta z = d_{33} E_z L_z$
 Quer-Effekt: $\Delta x = d_{31} E_z L_x$
 $\Delta y = d_{31} E_z L_y$



Scher-Effekt: $\Delta z = d_{15} E_x L_x$

The shear width Δz depends on the shear-piezoelectric constant k_{15} , the electric field in x-direction E_x , and the thickness in x-direction d , and is given by:

$$\Delta z = k_{15} E_x d_{\text{total}} = k_{15} E_x 4d = 4k_{15} \frac{\Delta U}{d} d = 4k_{15} \Delta U$$

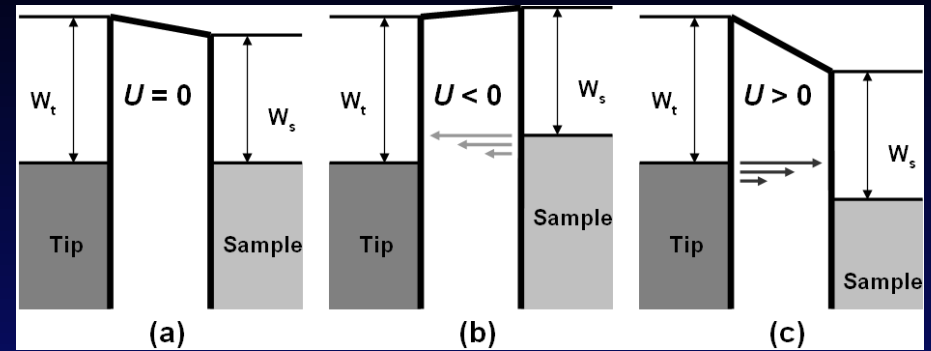
For a voltage of $U = \pm 400$ V the step width is $\Delta z_{\text{coarse}} = 1.056 \mu\text{m}$.



$$\Delta Z_{\text{fine}} \geq \Delta Z_{\text{coarse}}$$

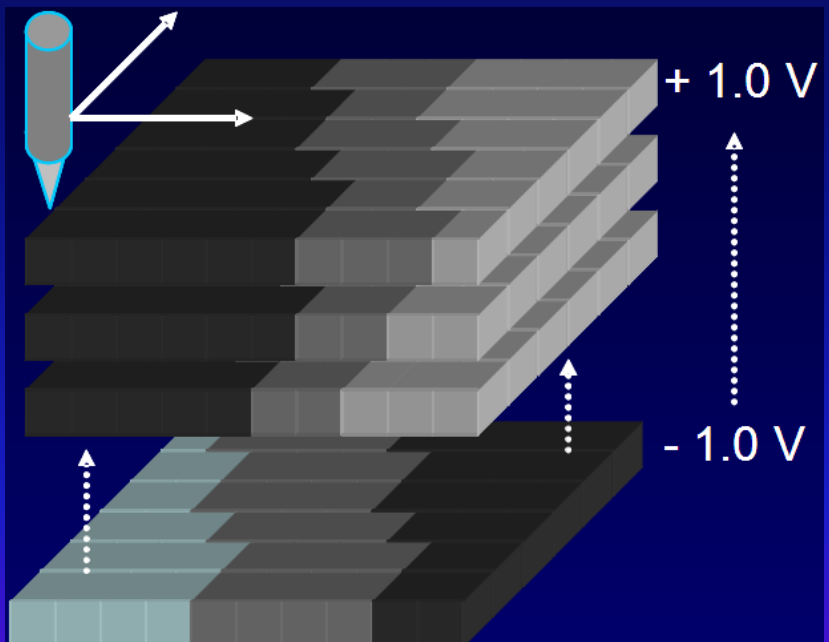
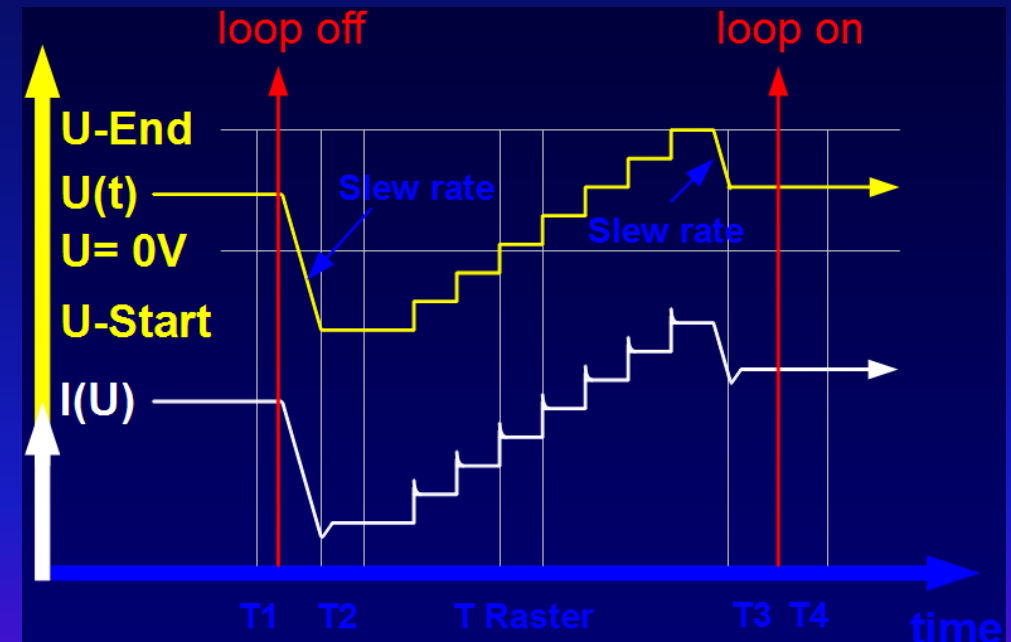
Scanning Tunneling Spectroscopy

Working Principle



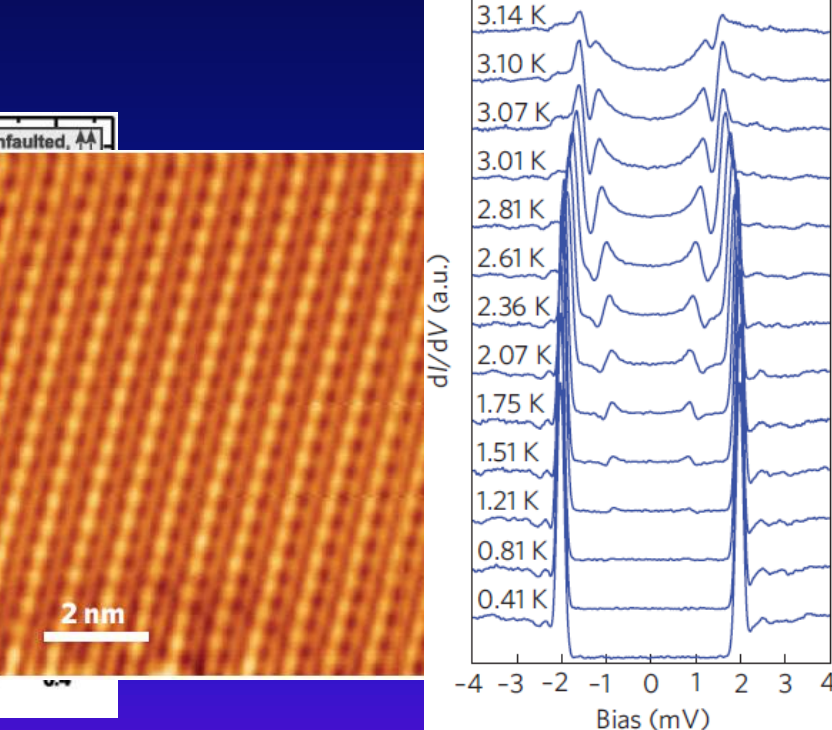
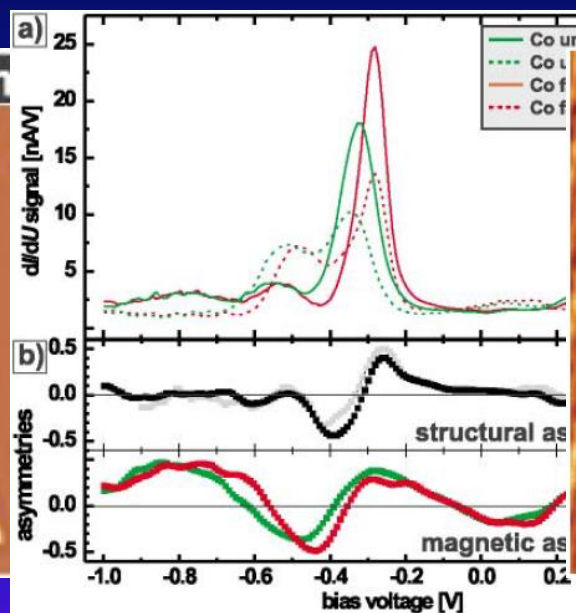
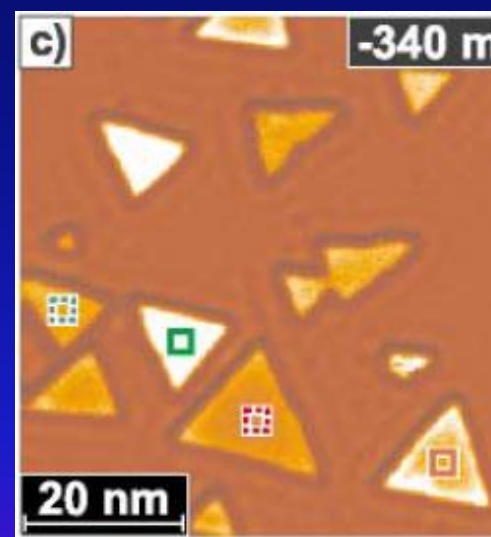
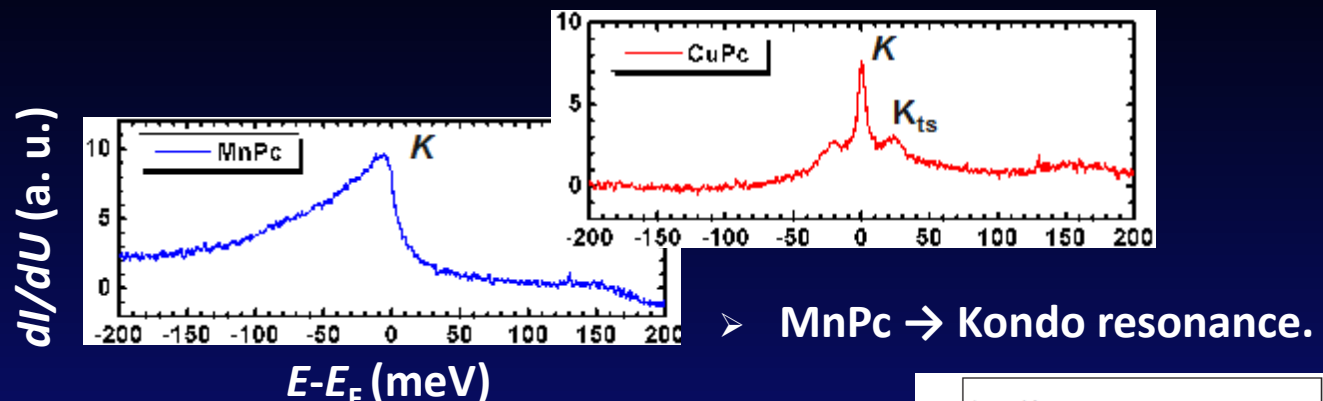
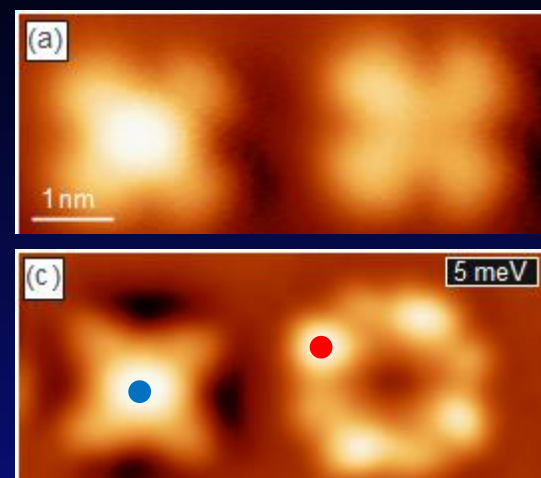
$$I \propto \int_0^{eU} \rho_s(\vec{r}_0, E_F + \varepsilon) \cdot \rho_t(E_F - eU + \varepsilon) d\varepsilon$$

$$\frac{dI}{dU} \propto \rho_s(\vec{r}_0, E_F + eU)$$



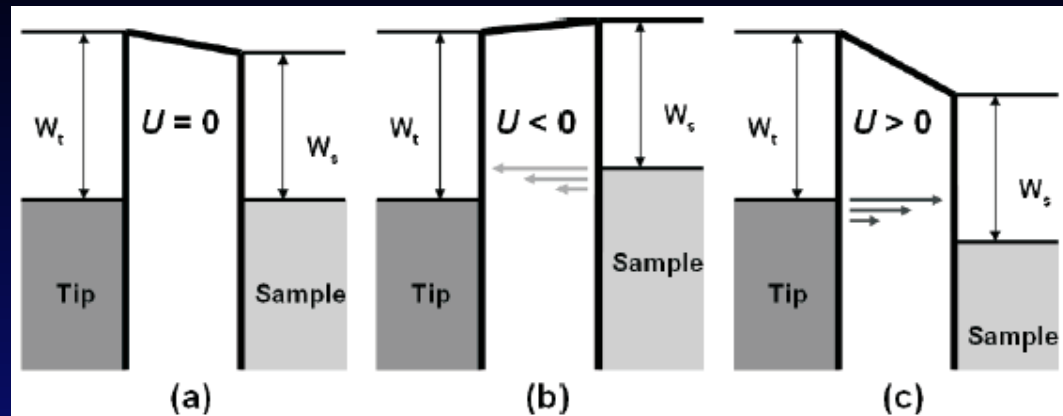
Scanning Tunneling Spectroscopy

Working Principle



Scanning Tunneling Spectroscopy

Working Principle



$$I \propto \int_0^{eU} \rho_s(E_F + \epsilon) \cdot \rho_t(E_F - eU + \epsilon) \cdot T(\epsilon, U, s) d\epsilon.$$

In the framework of a semi-classical WKB-approximation

$$T(E, U, s) \cong \exp [-2\kappa(E, U, s)],$$

$$\frac{dI}{dU}(U, s) \propto \rho_s(E_F + eU) \cdot \rho_t(E_F) \cdot T(eU, U, s)$$

$$+ \int_0^{eU} \rho_s(E_F + \epsilon) \cdot \rho_t(E_F + \epsilon - eU) \cdot \frac{d}{dU} T(\epsilon, U, s) d\epsilon$$

$$+ \int_0^{eU} \rho_s(E_F + \epsilon) \cdot T(\epsilon, U, s) \cdot \frac{d}{dU} \rho_t(E_F + \epsilon - eU) d\epsilon.$$

$$\kappa(E, U, s) = \sqrt{\frac{2m}{\hbar^2} (\bar{W} + \frac{eU}{2} - (E - E_{||}))}.$$

+ \bar{W} is the effective tunnel distance and $\bar{W} = (W_s + W_t)/2$ the average

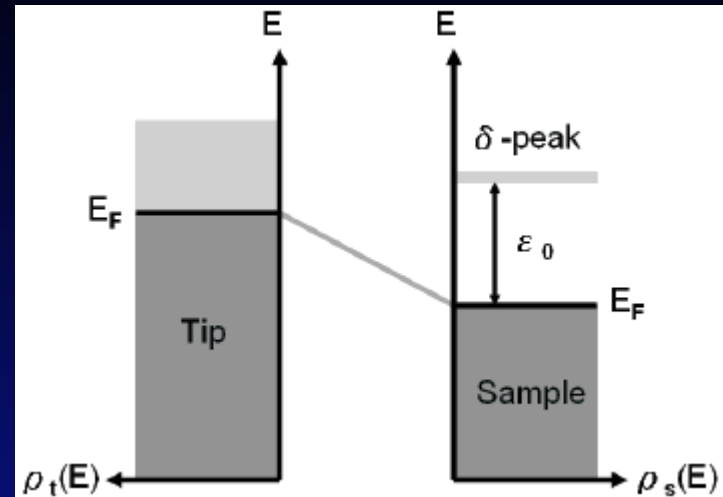
+ The decay constant $\kappa(\epsilon, U, k_{||})$ becomes minimal at a certain energy

ϵ_{min} for states that have a vanishing wave vector parallel to the surface ($k_{||} = 0$).

In the first term, we have the LDOS $\rho_s(E_F + eU)$ of the sample. Assuming a constant or weakly varying LDOS ρ_t of the tip, the third term can be neglected. The second term mainly contributes at high bias voltage due to the increase of the transmission coefficient T at high bias voltages.

Scanning Tunneling Spectroscopy

Working Principle



$$\frac{dI}{dU}(U) \propto \frac{1}{k_B T} \cdot \frac{1}{\cosh^2(\frac{\epsilon_0 + eU}{2k_B T})}. \quad \rho_s(\epsilon) = A\delta(\epsilon - \epsilon_0)$$

The differential tunnel conductance has a pronounced maximum at $-eU = \epsilon_0$ and the dI/dU signal can be approximated by a Gaussian line shape with full width at half maximum (FWHM) of $2\sigma = 3k_B T/e$.

$$\Delta E = 3k_B T.$$

A high energy resolution can only be achieved at low temperatures and an estimation leads to $\Delta E \approx 1$ meV for $T = 4$ K.

$$I = \frac{2\pi e}{\hbar} \int_{-\infty}^{\infty} [f(\epsilon + eU) - f(\epsilon)] \cdot |M_{\mu\nu}|^2 \cdot \rho_t(\epsilon + eU) \cdot \rho_s(\epsilon) d\epsilon. \quad \Delta E = \sqrt{\delta E_{therm}^2 + \delta E_{mod}^2} = \sqrt{(3k_B T)^2 + (2.5 \cdot eU_{mod})^2}.$$

Here U is the difference of the potentials of tip and sample, $\epsilon = E - E_F$ the relative energy of the electrode with respect to the Fermi level and $f(\epsilon) = [\exp(\epsilon/k_B T) + 1]^{-1}$ the Fermi-Dirac distribution. While looking at a small energy window, the tunnel matrix elements $M_{\mu\nu}$ are constant.

$$\frac{dI}{dU}(U) \propto |M_{\mu\nu}|^2 \cdot \rho_t \int_{-\infty}^{\infty} \left[\frac{(1/k_B T) \exp[(\epsilon + eU)/k_B T]}{(\exp[(\epsilon + eU)/k_B T] + 1)^2} \right] \cdot \rho_s(\epsilon) d\epsilon.$$

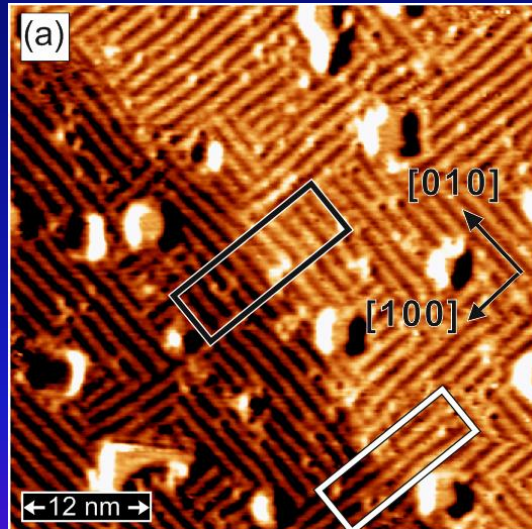
Quantum World at Atomic Scale: Spin-Polarized Scanning Tunneling Microscopy

Pin-Jui Hsu^{1,2} (徐斌睿)

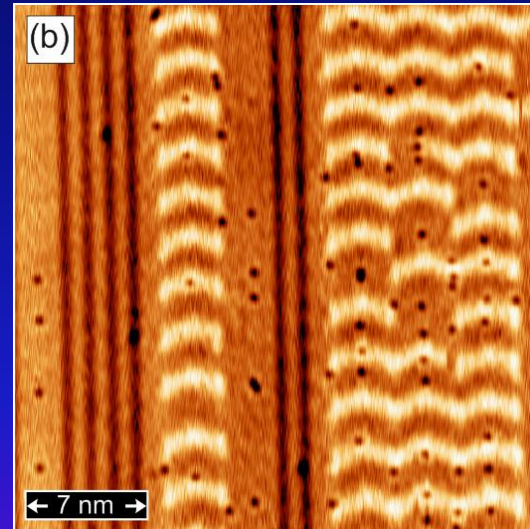
1. Institute of Applied Physics, University of Hamburg, Jungiusstrasse 11, D-20355 Hamburg, Germany

2. Department of Physics, National Tsing Hua University, No. 101, Section 2, Kuang-Fu Road, Hsinchu 30013, Taiwan

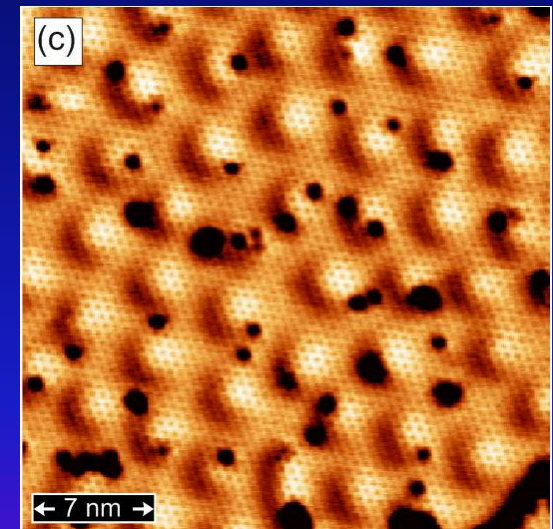
Fe-DL/ Rh(001)



Fe-TL/ Ir(111)



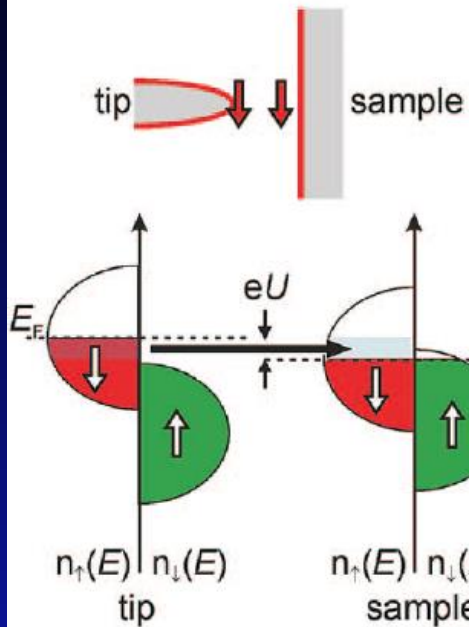
H/ Fe-DL/ Ir(111)



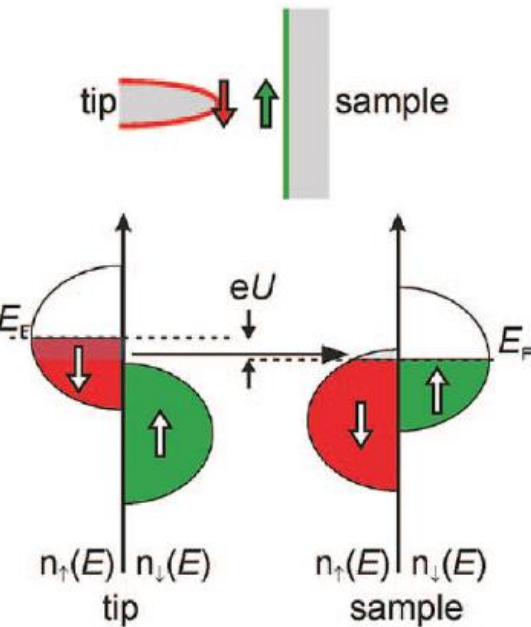
Spin-Polarized STM

Working Principle

parallel configuration



antiparallel configuration



$$I_{\text{SP}}(U_0) \propto I_0 \cdot [1 + P_{\text{tip}} \cdot P_{\text{sample}} \cdot \cos(\vec{m}_{\text{tip}}, \vec{m}_{\text{sample}})]$$

$$n_t = n_t^{\uparrow} + n_t^{\downarrow}, \quad n_s = n_s^{\uparrow} + n_s^{\downarrow}$$

$$m_t = n_t^{\uparrow} - n_t^{\downarrow}, \quad m_s = n_s^{\uparrow} - n_s^{\downarrow},$$

$$P_t = m_t/n_t, \quad P_s = m_s/n_s,$$

$$I(\vec{r}_0, U, \theta) = I_0(\vec{r}_0, U) + I_{\text{sp}}(\vec{r}_0, U, \theta)$$

$$= \frac{4\pi^3 C^2 \hbar^3 e}{\kappa^2 m^2} [n_t \tilde{n}_s(\vec{r}_0, U) + \vec{m}_t \tilde{m}_s(\vec{r}_0, U)]$$

where n_t is the non-spin-polarized LDOS at the tip apex, \tilde{n}_s is the energy-integrated LDOS of the sample, and \vec{m}_t and \tilde{m}_s are the corresponding vectors of the (energy-integrated) spin-polarized (or magnetic) LDOS

$$\tilde{m}_s(\vec{r}_0, U) = \int^{eU} \vec{m}_s(\vec{r}_0, E) dE,$$

with

$$\vec{m}_s = \sum \delta(E_\mu - E) \Psi_\mu^S(\vec{r}_0) \sigma \Psi_\mu^S(\vec{r}_0).$$

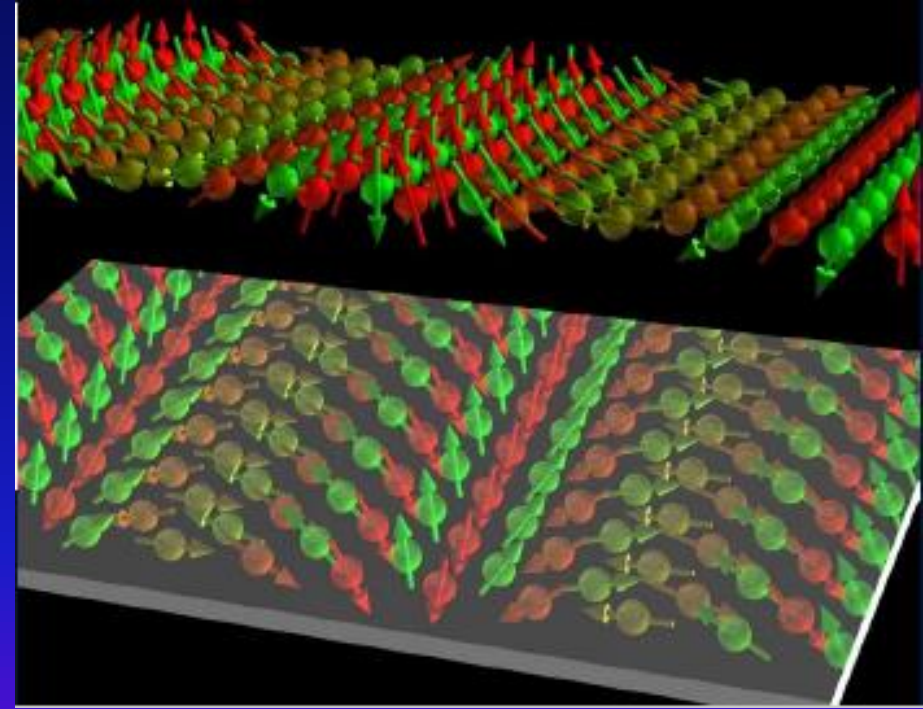
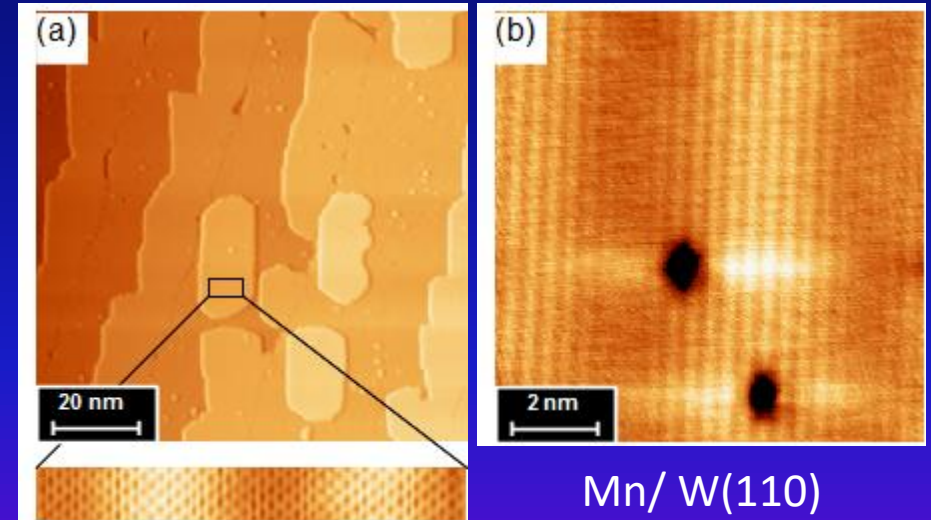
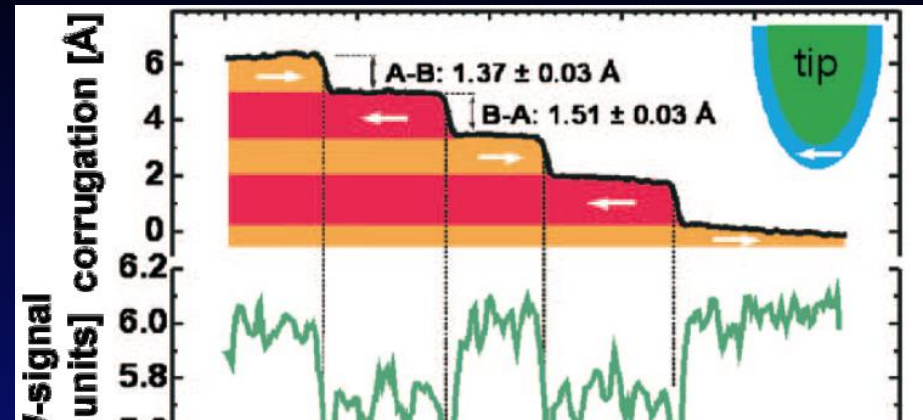
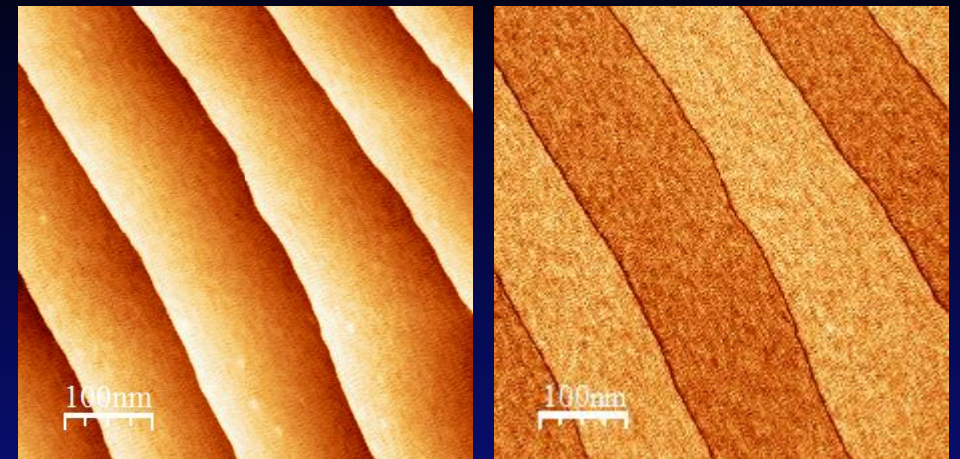
Ψ_μ^S denotes the spinor of the sample wave function

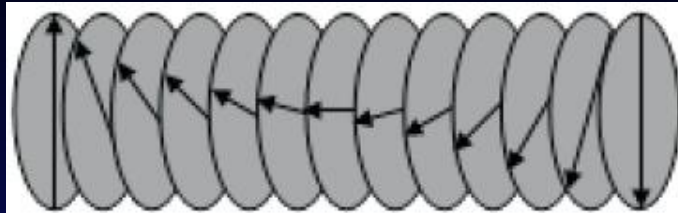
$$\Psi_\mu^S = \begin{pmatrix} \Psi_{\mu\uparrow}^S \\ \Psi_{\mu\downarrow}^S \end{pmatrix}$$

and σ is Pauli's spin matrix. As an important result, the spin-dependent contribution I_{sp} to the total tunneling current is found to scale with the projection of \tilde{m}_s onto \vec{m}_t , and therefore with the cosine of the angle θ between the magnetization directions of the two electrodes, in agreement with the limiting case of vanishing applied bias voltage

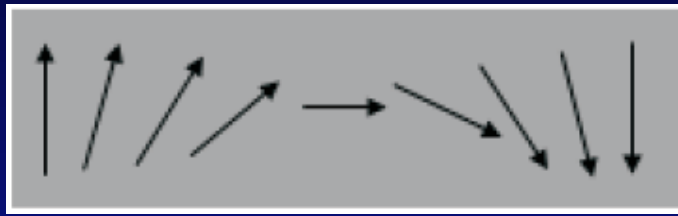
Spin-Polarized STM

Working Principle





Bloch Wall



Néel Wall

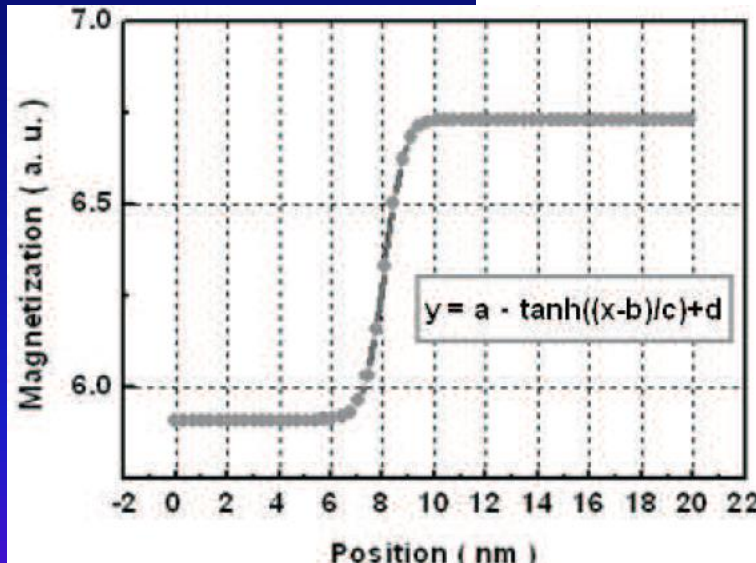
the exchange energy intends to make the wall wider in order to make the angle ϕ between adjacent spins become smaller and the anisotropy energy tries to make the wall thinner in order to reduce the number of spins aligning to non-easy axis directions. As a consequence of these two energy competition, there is a certain finite width and a certain spin structure of the magnetic domain wall.

Besides, the domain wall width can be expressed in the form of $\phi(x)$ dependence,

$$E_{ex} = E_{an} \Rightarrow J \frac{d\phi}{dx} = K \cos^2 \phi$$

$$\Rightarrow \sqrt{\frac{K}{J}} dx = \frac{d\phi}{\cos \phi}$$

$$\sqrt{\frac{K}{J}} x = \tanh^{-1}(\tan \phi)$$

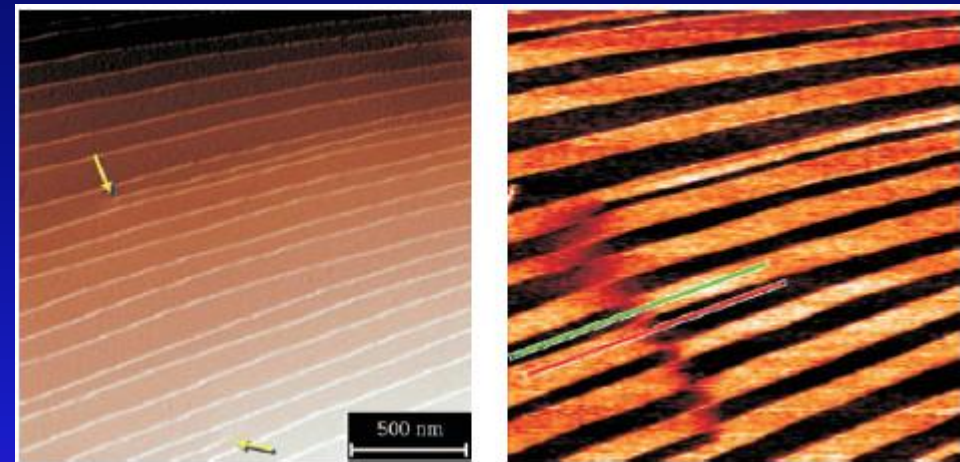


Spin-Polarized STM

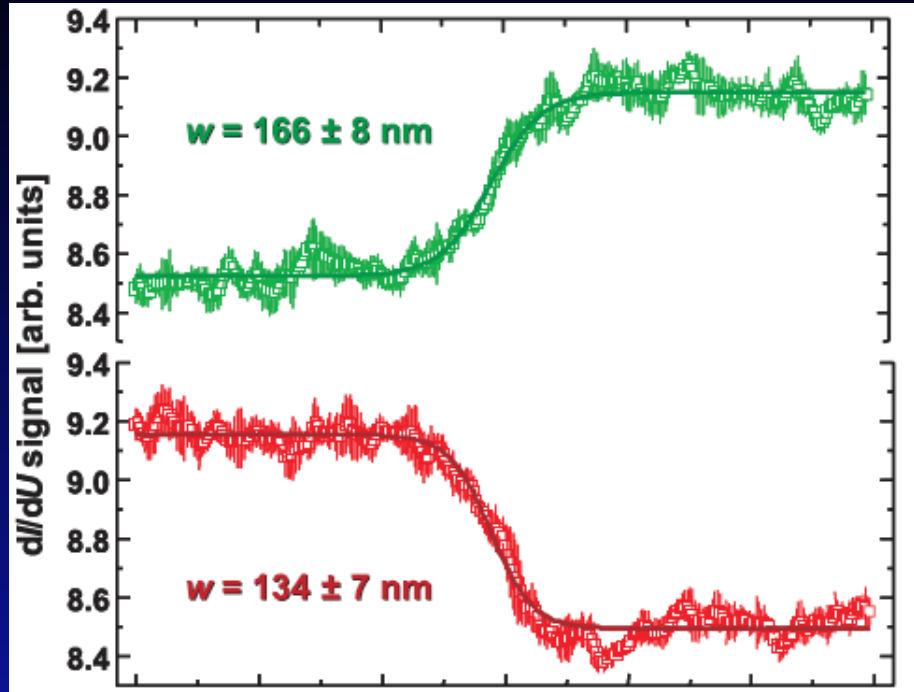
Magnetic Domain Wall, AFM Cr(001)



Cr(001)



$$y(x) = y_0 + y_{sp} \tanh\left(\frac{x - x_0}{w/2}\right)$$



$w = 2 \sqrt{A/k}$ the domain-wall width w is one-to-one determined by the ratio A/k , where A is the so-called exchange stiffness and k is the effective anisotropy energy density.

For instance, we may assume that $A_{Cr} = 1 \times 10^{-11} \text{ J/m}$ and $k_{Cr} = 1.77 \times 10^3 \text{ J/m}^3$. We believe that in consideration of the fact that the “Stoner parameter” I of Cr, $I_{Cr} = 0.58\text{--}0.68 \text{ eV}$,^{23–25} is considerably smaller than $I_{Fe} = 0.88 \text{ eV}$,²⁶ this assumption for A_{Cr} is justified.

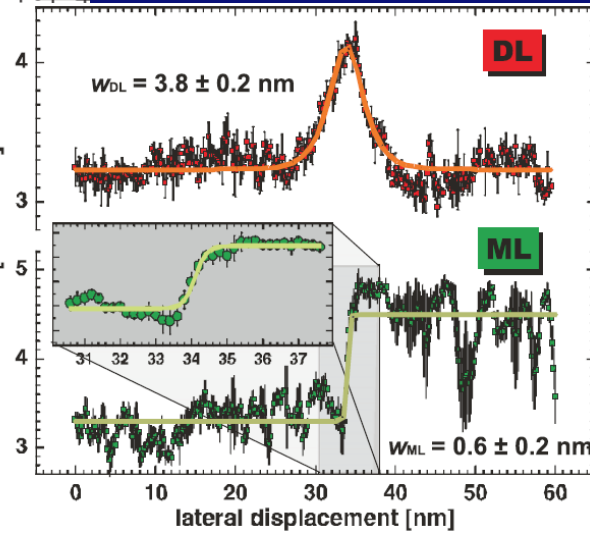
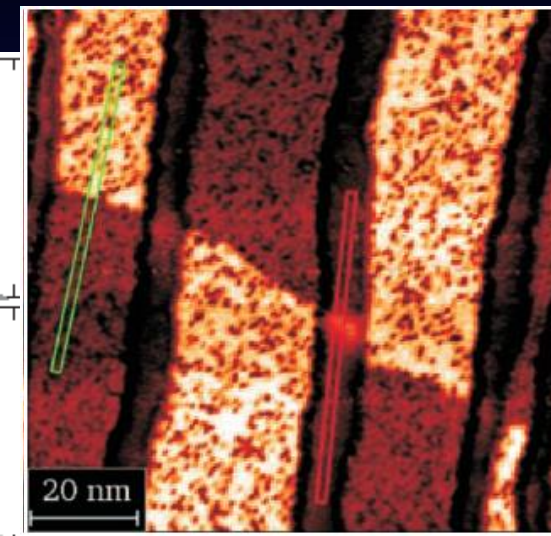
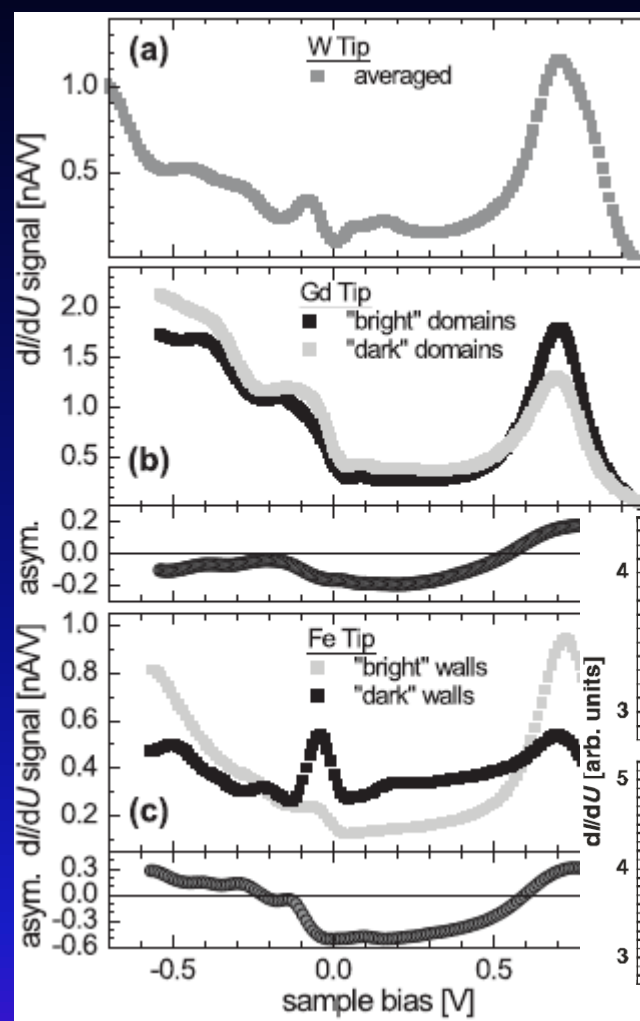
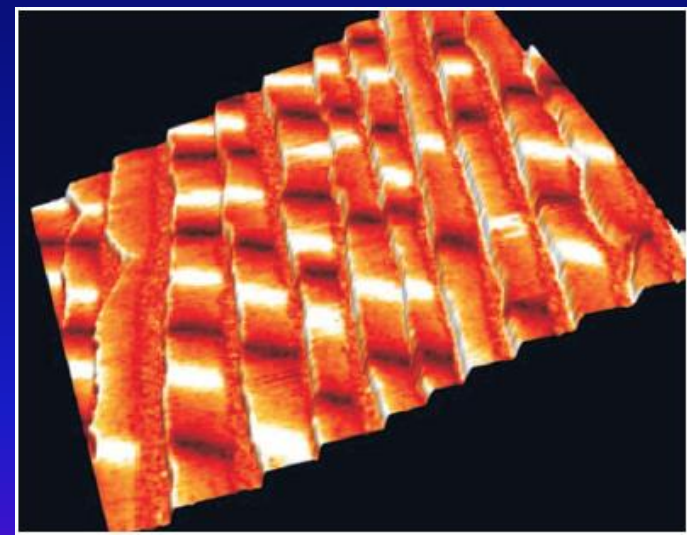
R. Wiesendanger, Rev. Mod. Phys., 81, 1495 (2009)

Spin-Polarized STM

Magnetic Domain Wall, FM Fe-DL/W(110)



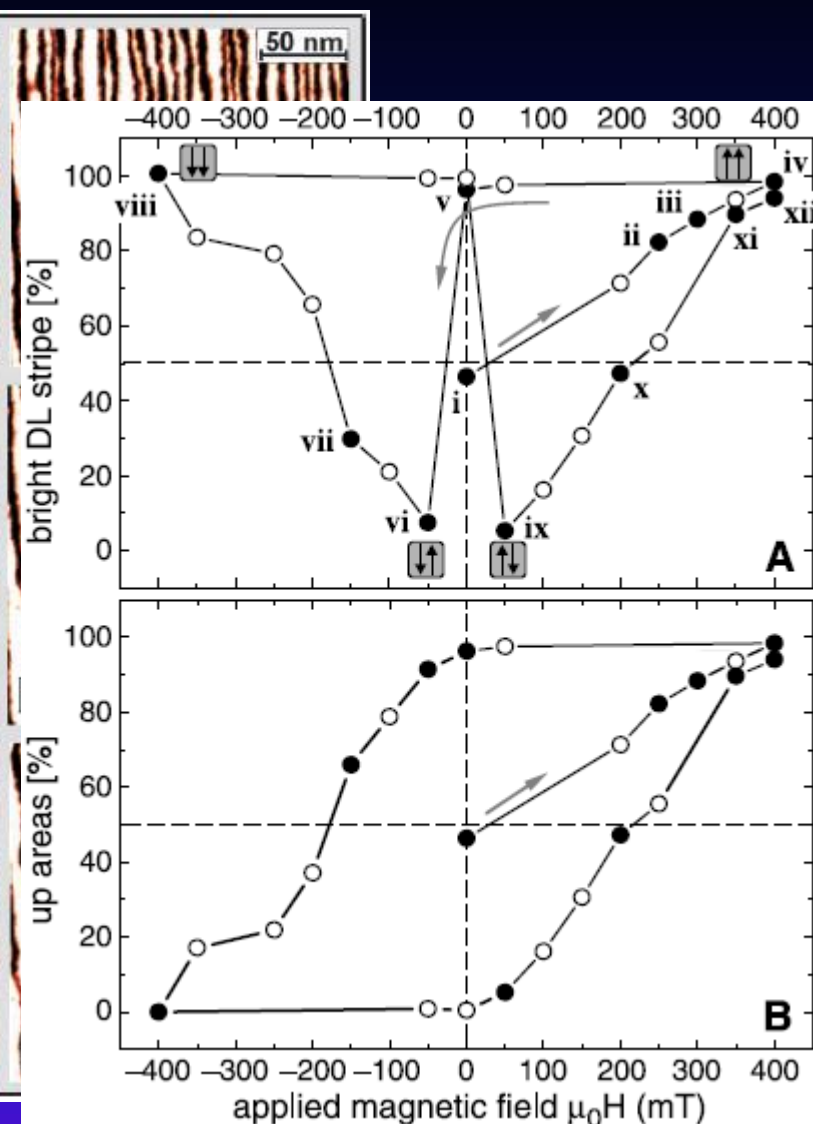
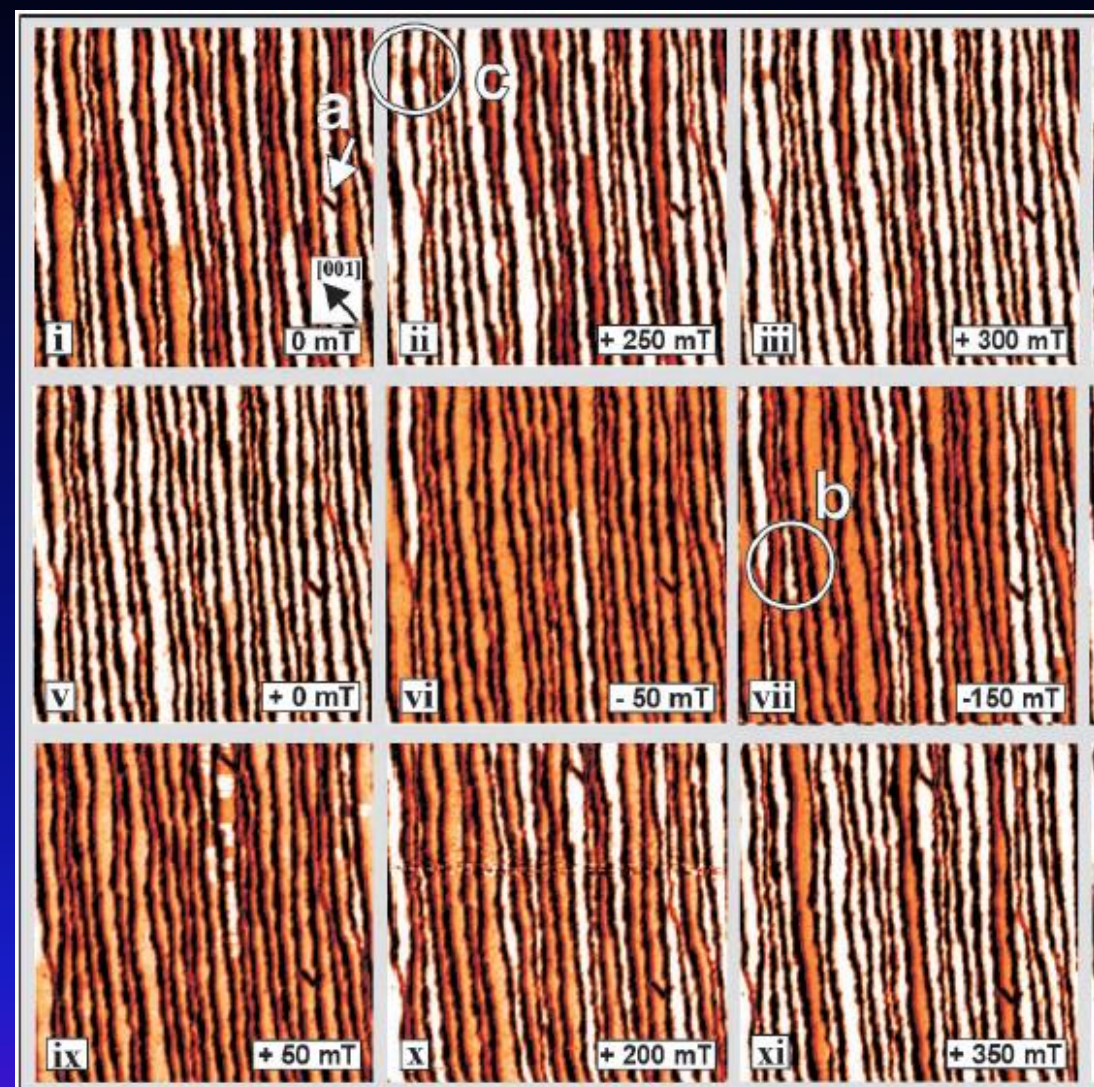
國立清華大學
NATIONAL TSING HUA UNIVERSITY



R. Wiesendanger, Rev. Mod. Phys., 81, 1495 (2009)

Spin-Polarized STM

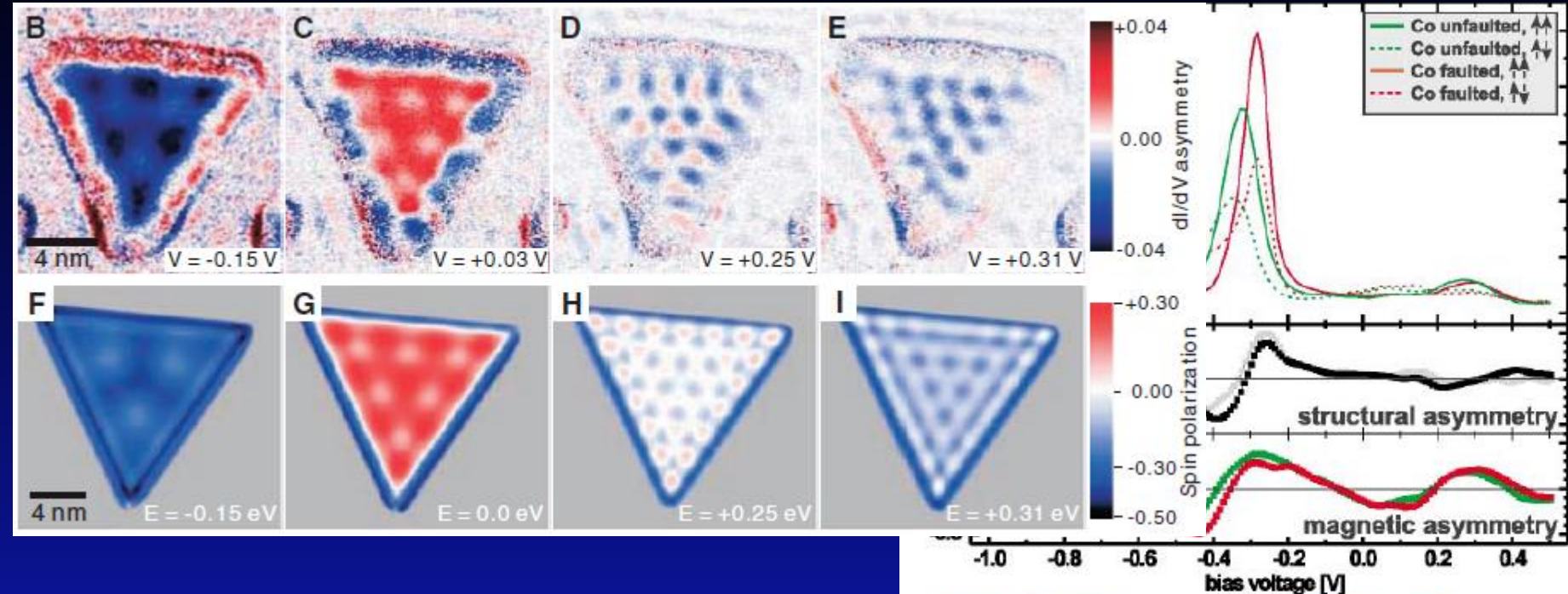
Magnetic Domain Wall, FM Fe-DL/W(110)



O. Pietzsch *et al.*, Science, 292, 2053 (2001)

Spin-polarized States

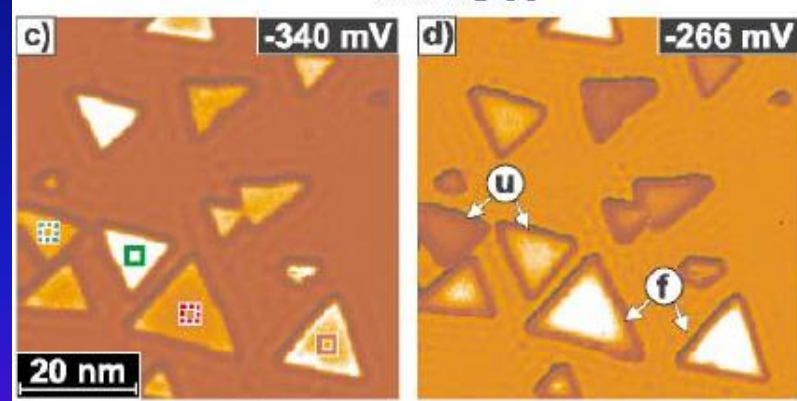
Spin-polarized Surface State, FM Co-DL/Cu(111)



L. Diekhöner *et al.*, Phys. Rev. Lett., 90, 236801 (2003)

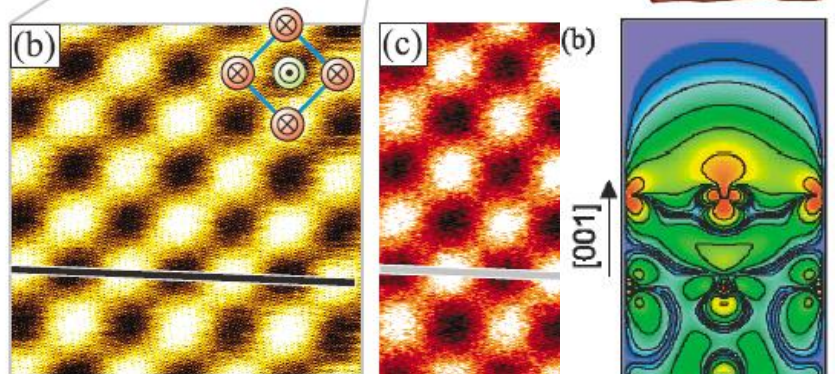
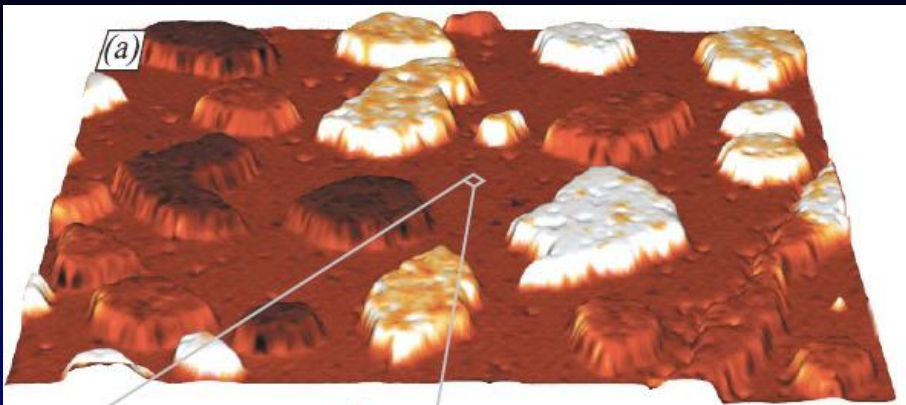
O. Pietzsch *et al.*, Phys. Rev. Lett., 92, 057202 (2004)

H. Oka *et al.*, Science, 327, 843 (2010)

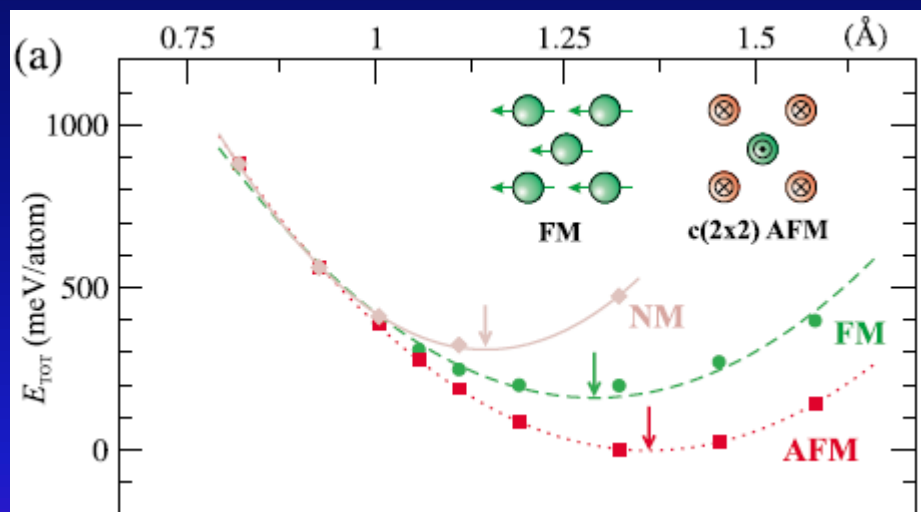
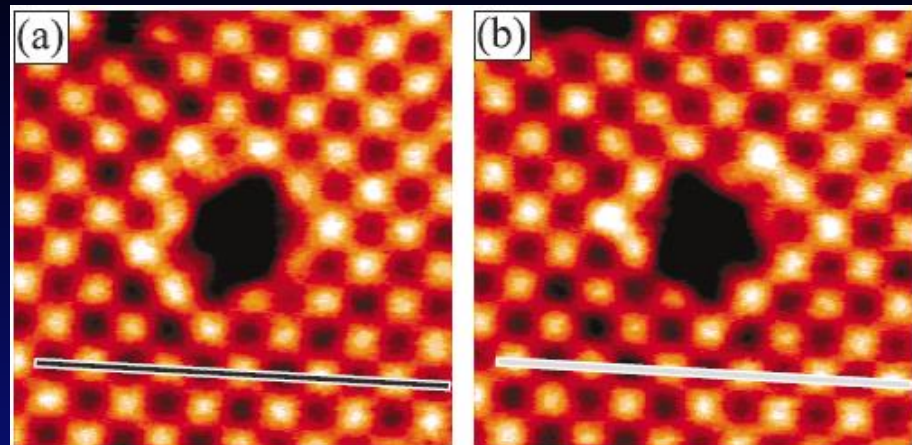
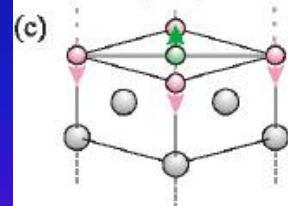


Spin-Polarized STM

Atomic Spin Resolution, AFM Fe-ML/W(001)

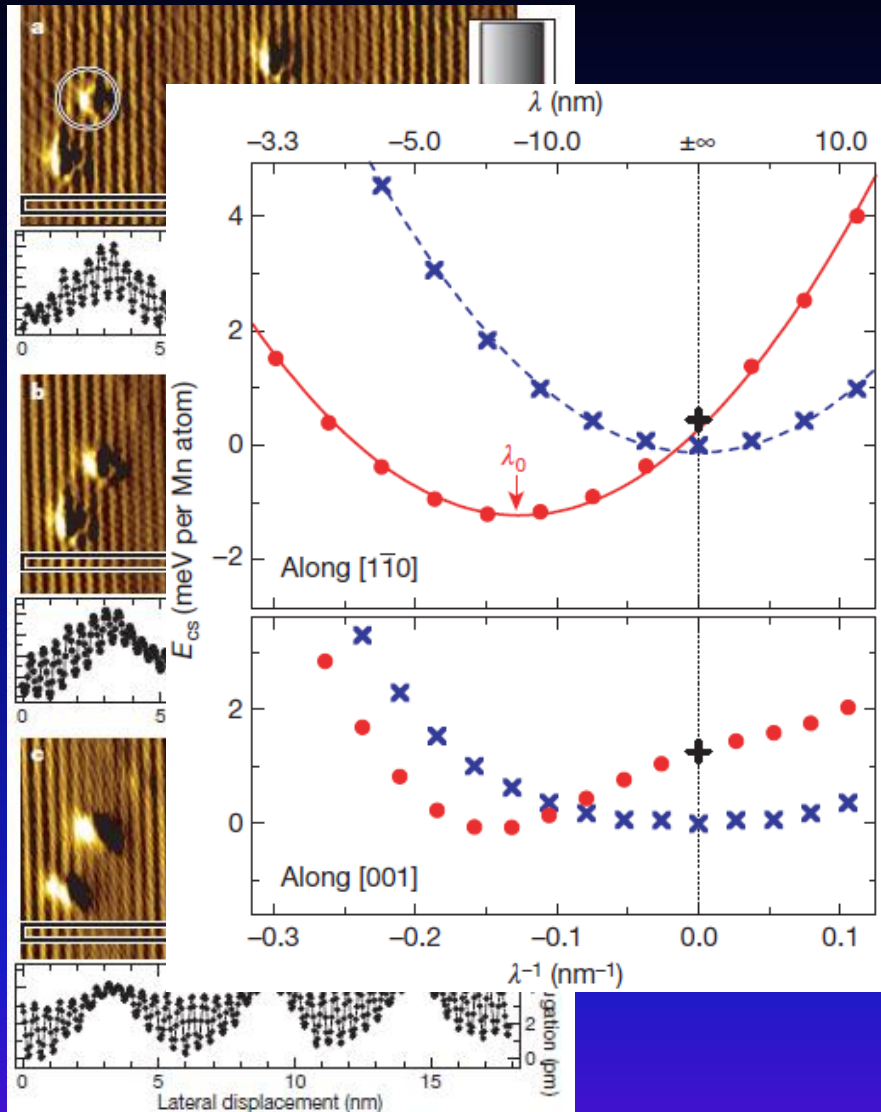
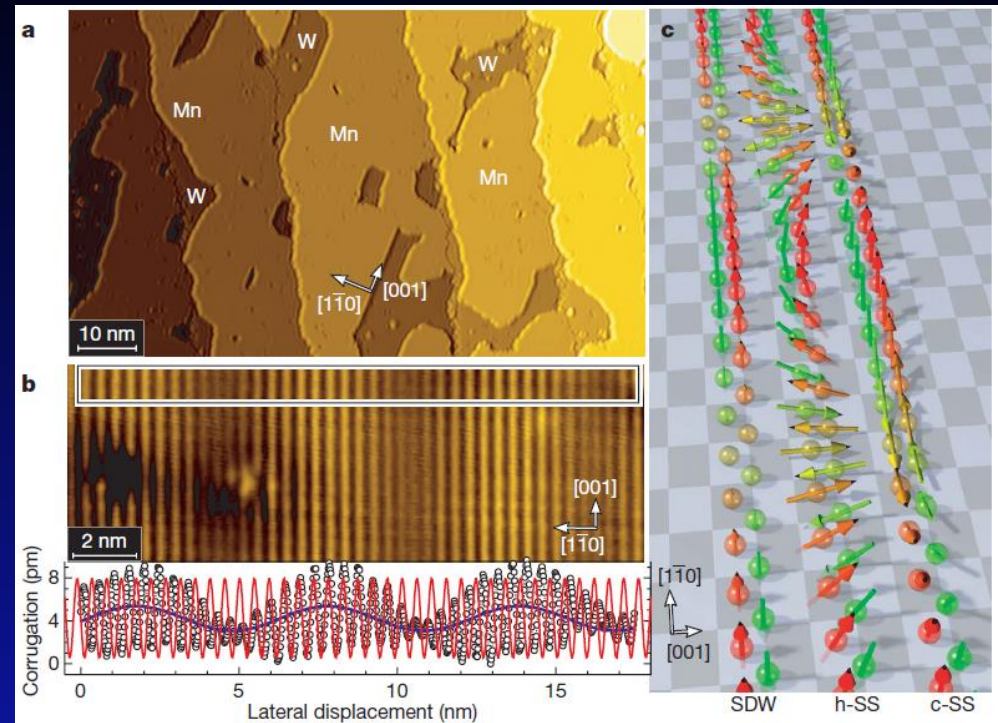


A. Kubetzka *et al.*, Phys. Rev. Lett., 90, 236801 (2003)



Spin-Polarized STM

Atomic Spin Resolution, AFM Mn-ML/W(110)



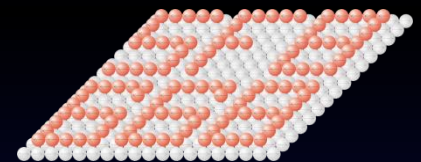
This is the Dzyaloshinskii–Moriya interaction^{3,4}, DMI,

$$E_{DM} = \sum_{i,j} D_{ij} \cdot (S_i \times S_j)$$

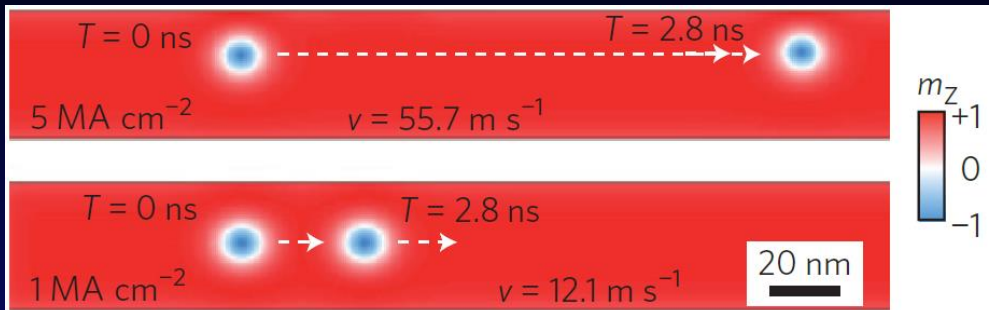
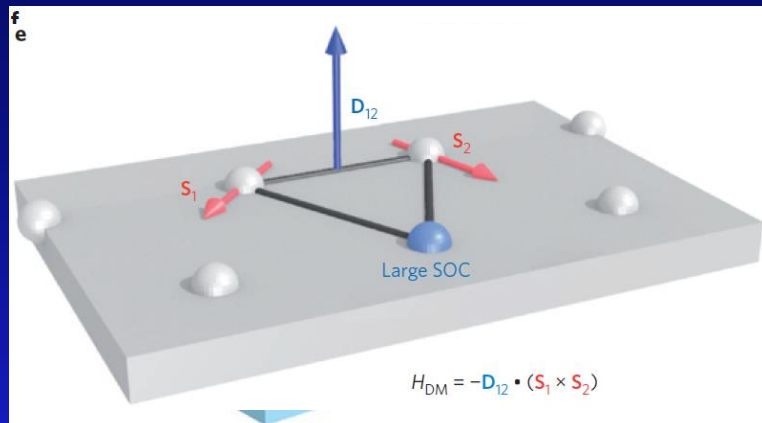
M. Bode *et al.*, Nature, 447, 190 (2007)

Magnetic Skyrmion

Dzyaloshinsky-Moriya Interaction



$$E_{\text{DM}} = - \sum_{ij} \mathbf{D}_{ij} (\mathbf{S}_i \times \mathbf{S}_j)$$



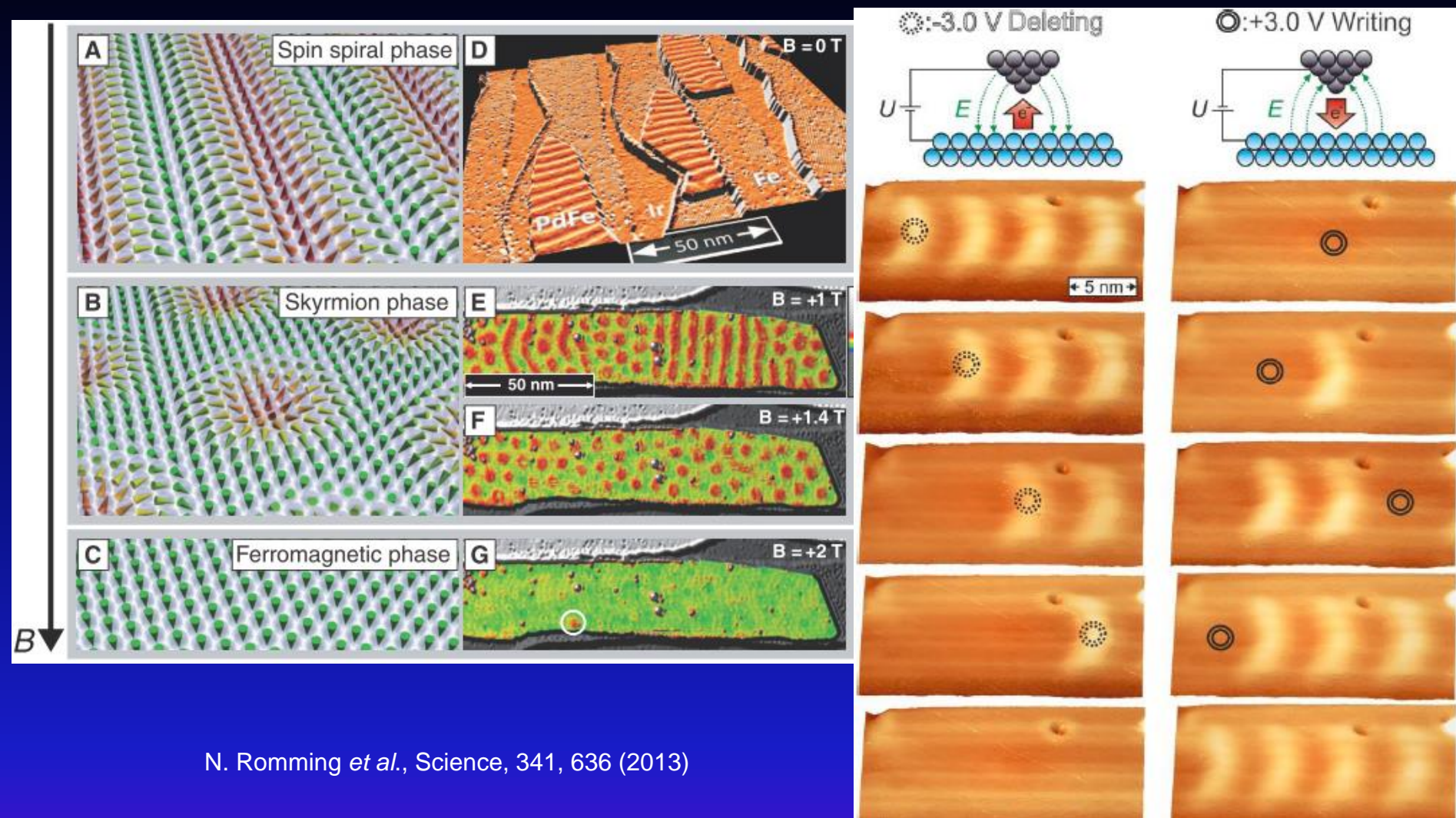
- DMI has the dominant contributions to formation of magnetic skyrmion spin texture.

A. Fert, V. Cros, and J. Sampaio, Nature Nano., 8, 152 (2013)

- The current density required to move skyrmions has 5~6 order of magnitudes smaller than DW movement.
- Non-trivial topology and lower depinning currents lead to low energy consumption.

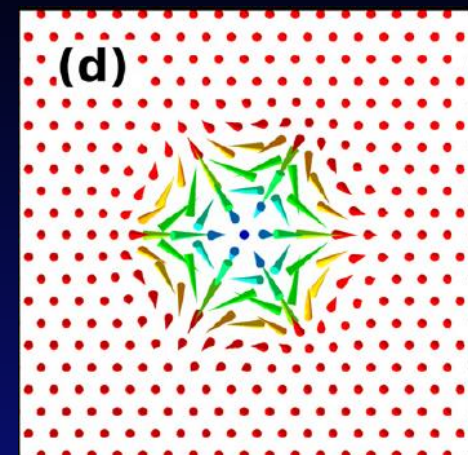
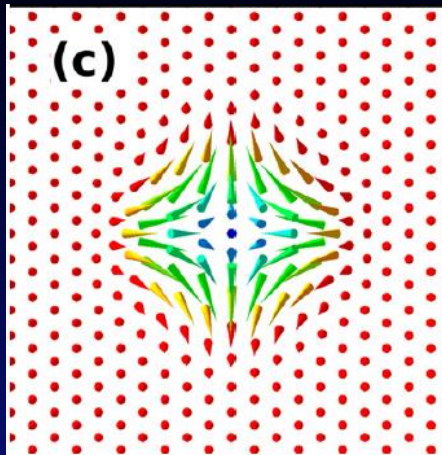
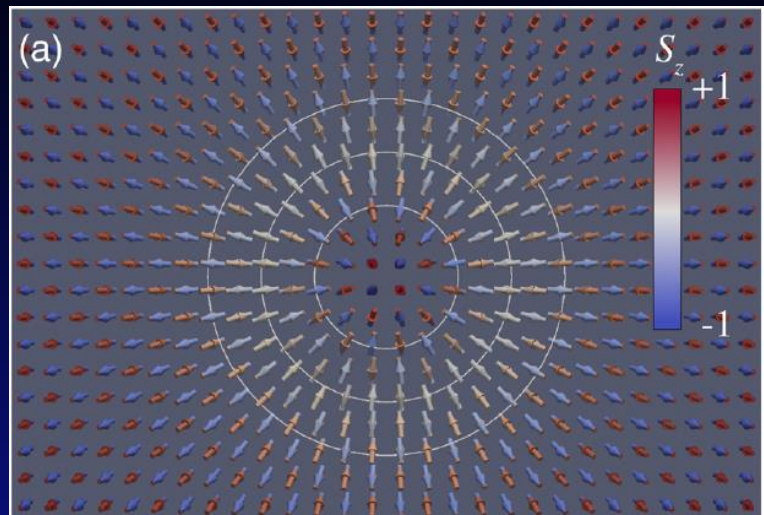
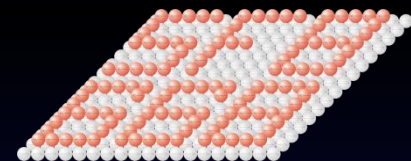
Spin-Polarized STM

Magnetic Phase transition, Magnetic Skyrmions

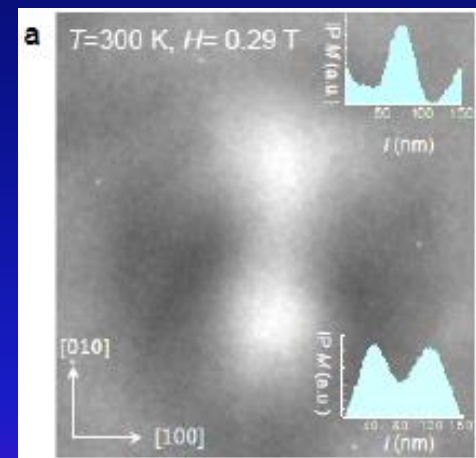
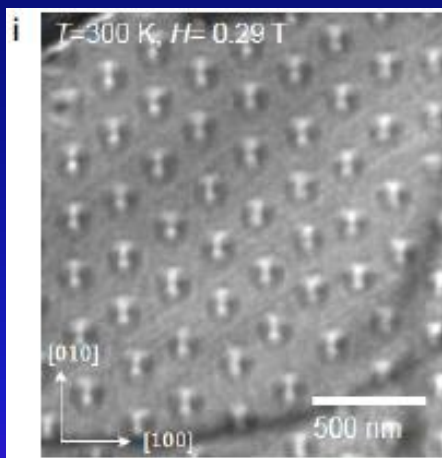
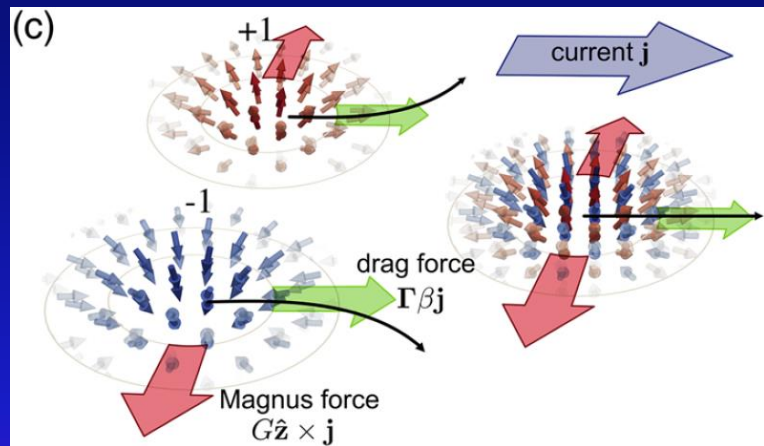


Magnetic Skyrmion

AFM skyrmion; Antiskyrmion; $|Q| > 1$



B. Dupé, C. N. Kruse, T. Dornheim, and S. Heinze, New. J. Phys., 18, 055015 (2016)

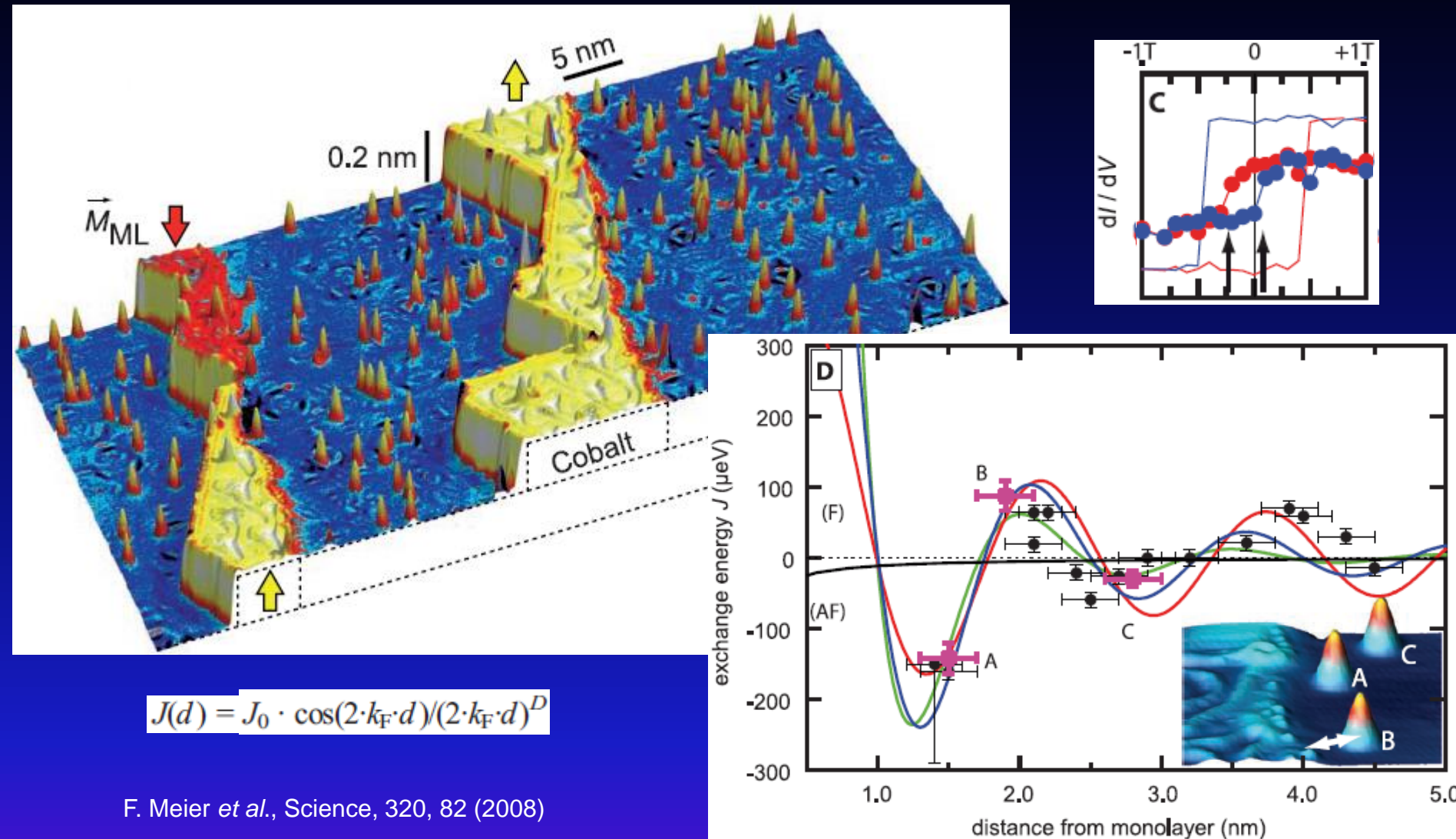


J. Barker, and O. A. Tretiakov, Phys. Rev. Lett., 116, 147203 (2016)

A. K. Nayak, V. Kumar, P. Werner, E. Pippel, R. Sahoo, F. Damay, U. K. Roßler, C. Felser, and S. P. Parkin, Nature, 548, 561 (2017)

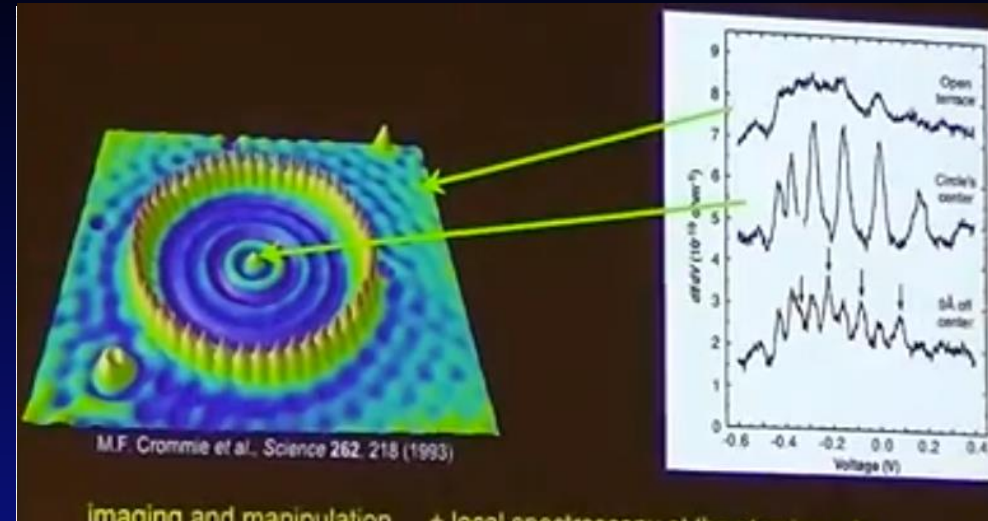
Single-Atom Magnetometry

SP-STM/STS with B field, Co atoms/Pt(111)



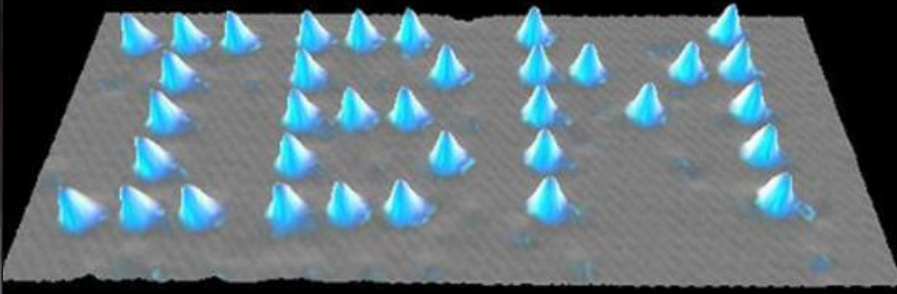
Single-Atom Magnetometry

Moving Single Atoms

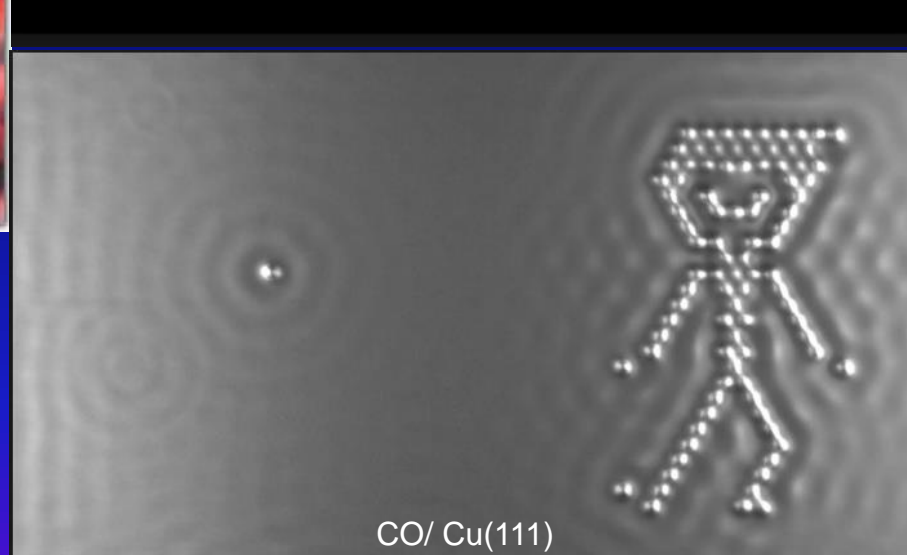


75 Fe/ Cu(111)

M. F. Crommie et al., Science, 262, 218 (1993)



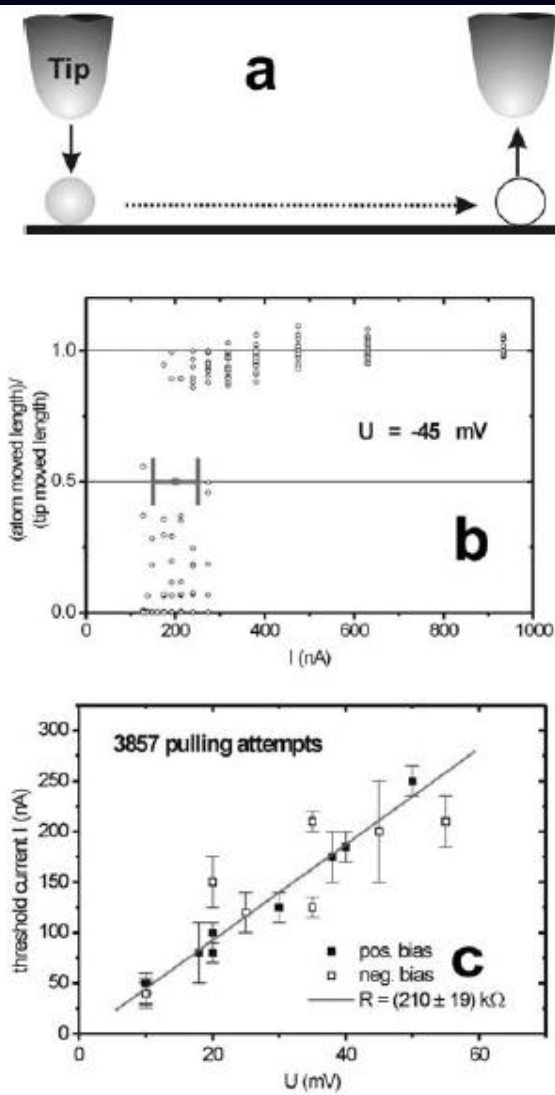
34 Xe / Ni(110)



CO/ Cu(111)

Single-Atom Magnetometry

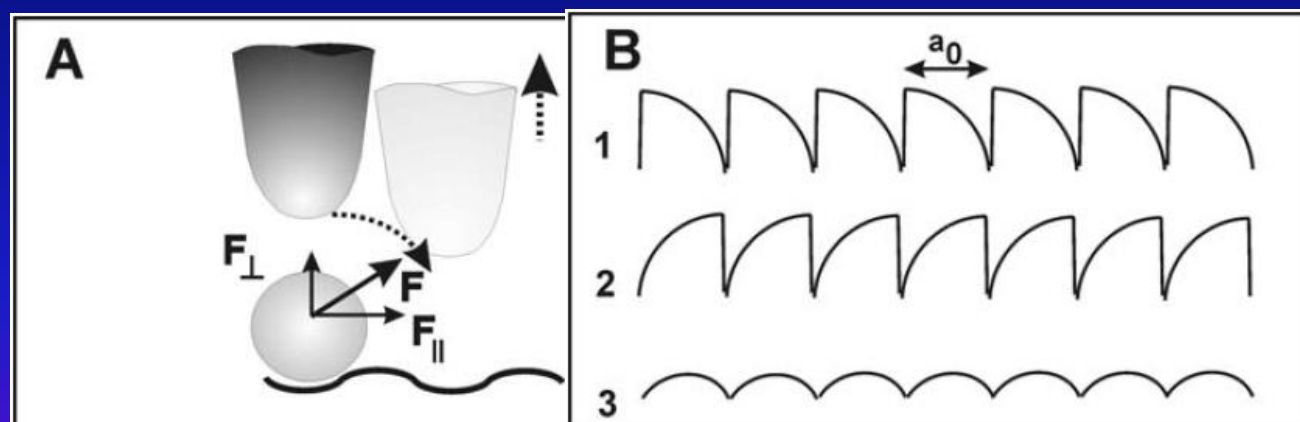
Moving Single Atoms, Lateral Movement



In case of a silver atom manipulation on Ag(111), $R_t = 184 \pm 8 \text{ k}\Omega$ is necessary³⁷. This R_t corresponds to a distance of 1.9 Å between the edges of van-der-Waals radii of tip-apex and manipulated atom. Since the atomic orbitals of tip-apex and manipulated atoms are overlapping at this distance, a weak chemical bond is formed. The attractive force used in the “pulling” manipulation is originated from this chemical nature of interaction.

S. W. Hla, J. Vac. Sci. & Tech. B,
23, 1351 (2005)

Three basic LM modes, “pushing”, “pulling” and “sliding”, has been distinguished⁵. In the “pulling” mode, the atom follows the tip due to an attractive tip-atom interaction. In the “pushing” mode, a repulsive tip-atom interaction drives the atom to move in front of the tip. In the “sliding” mode, the atom is virtually bound to or trapped under the tip and it moves smoothly across the surface together with the tip.



Single-Atom Magnetometry

Moving Single Atoms, Vertical Manipulation

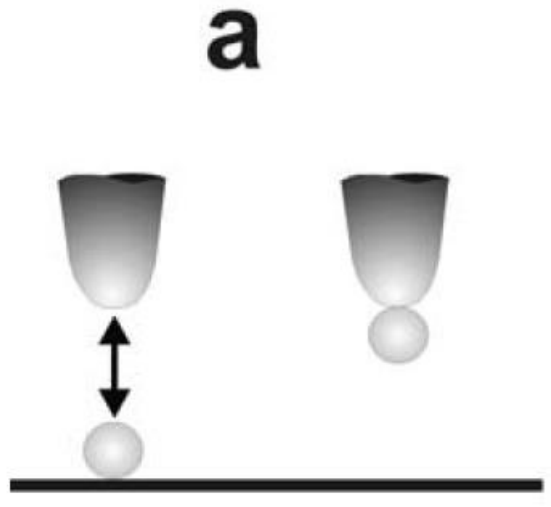
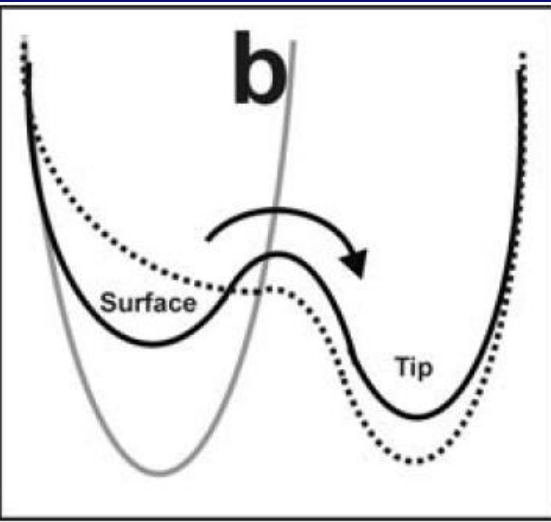
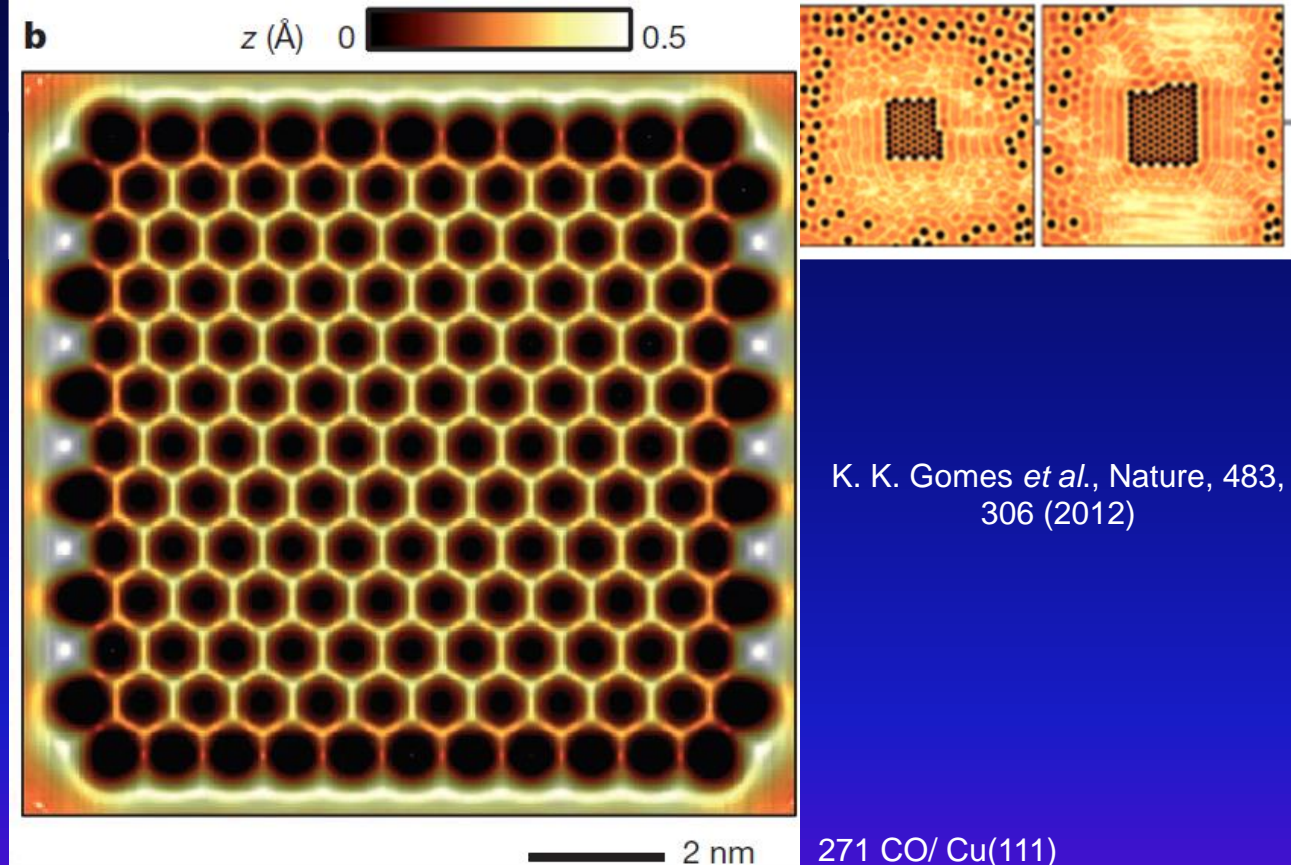
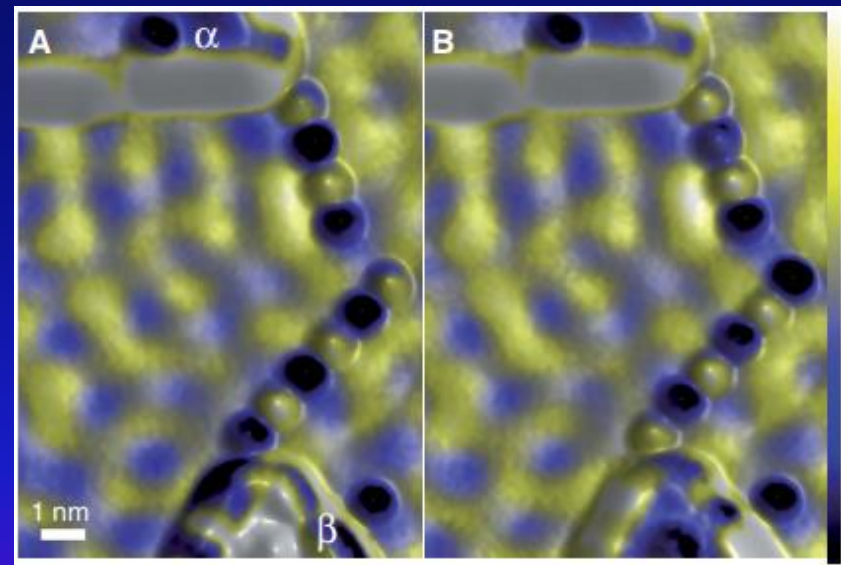
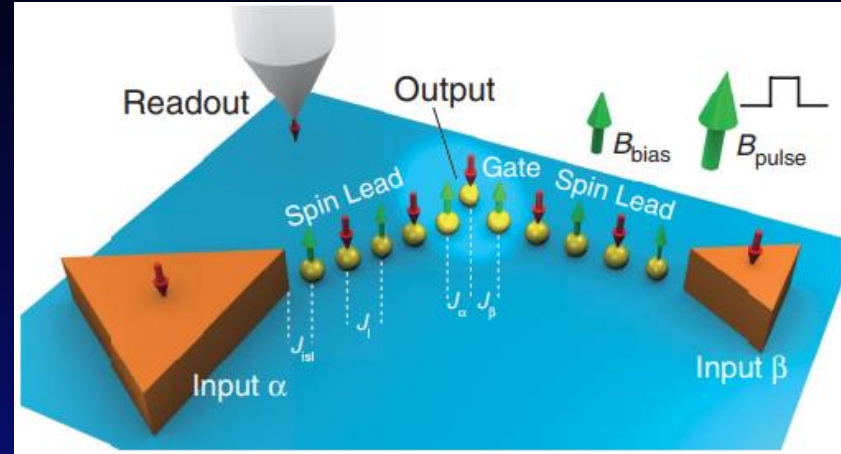
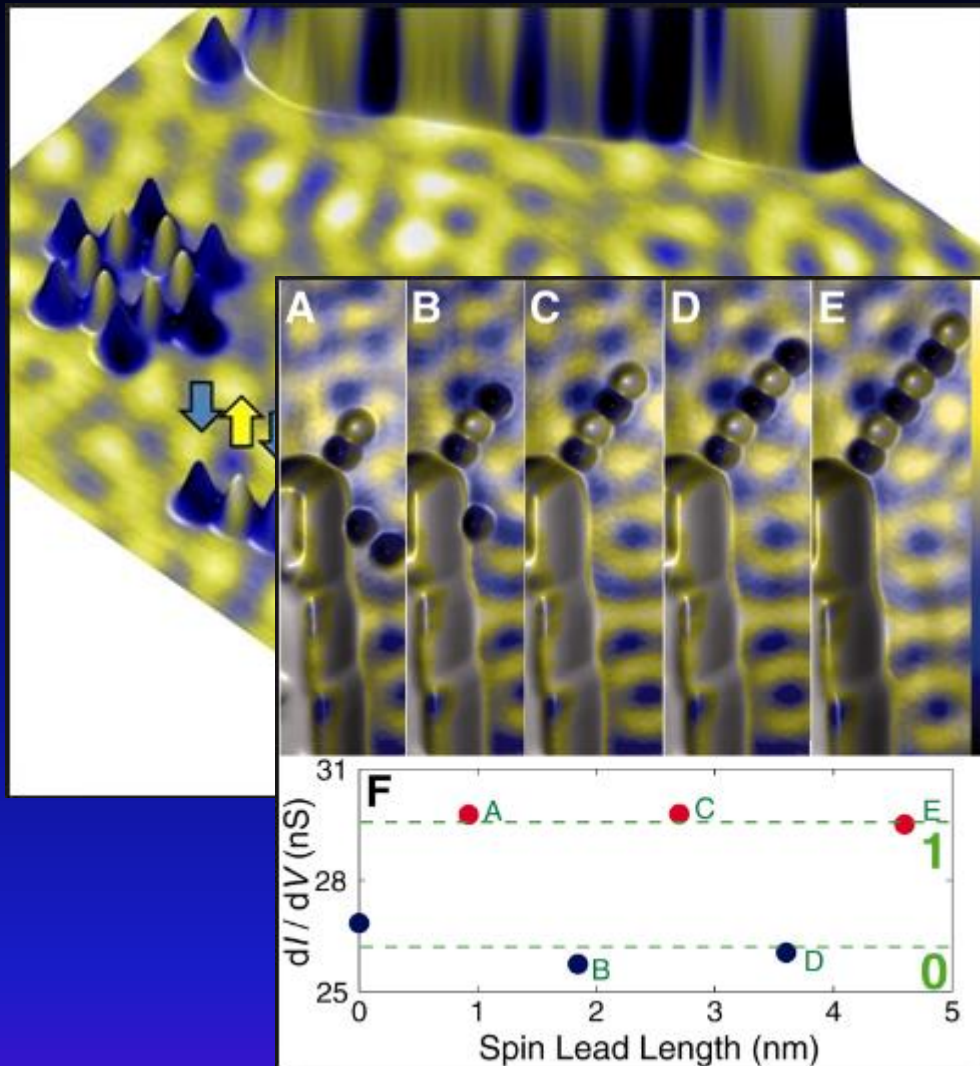
a**b**

Fig. 8. Vertical manipulation (VM). (a) A schematic drawing shows the process. (b) The double-potential well model. The black (solid), dash and gray curves represent the shape of potentials (the well shapes are working assumptions) at an image-height, under an electric field, and at the tip-atom/molecule contact, respectively.

b

Moving Single Atoms

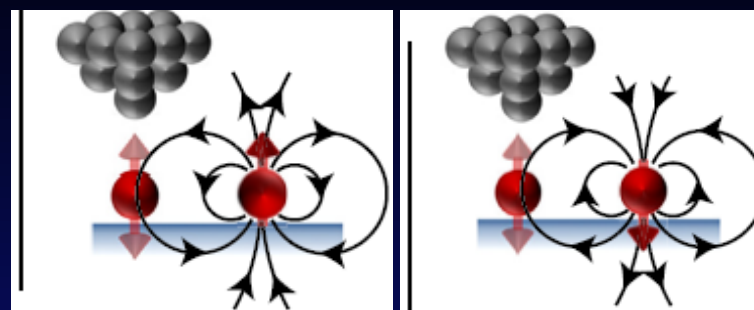
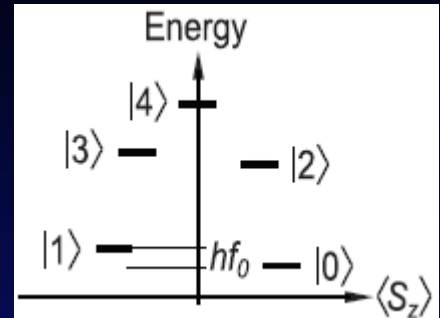
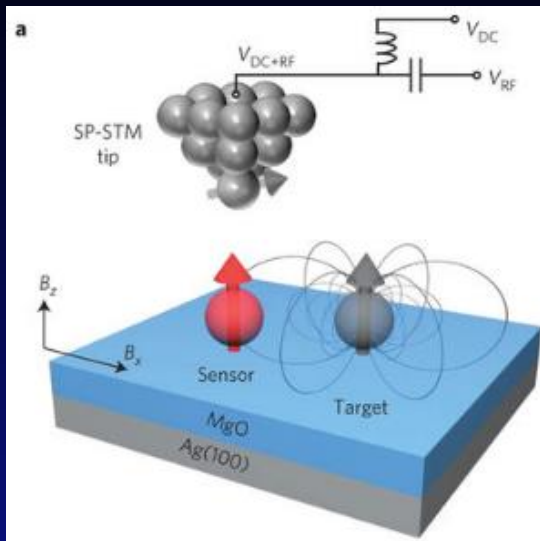
Spin Logic Operations



A. Khajetoorians *et al.*, Science, 332, 1062 (2011)

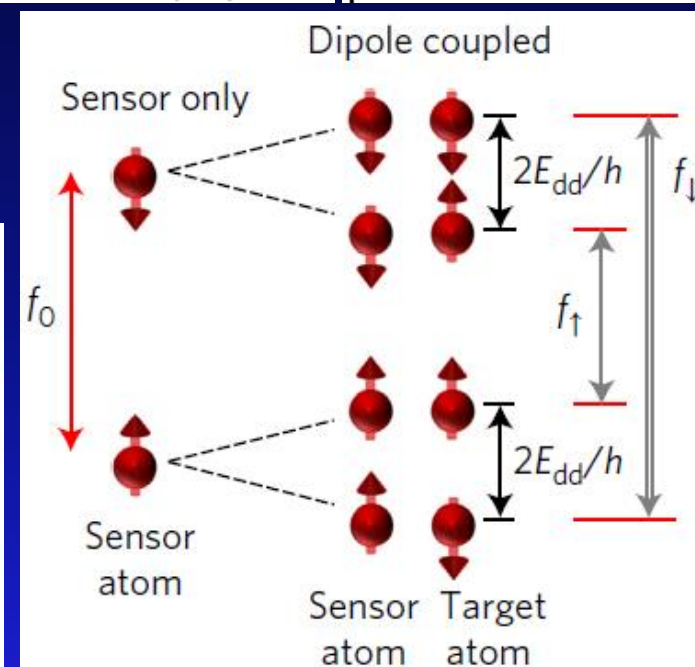
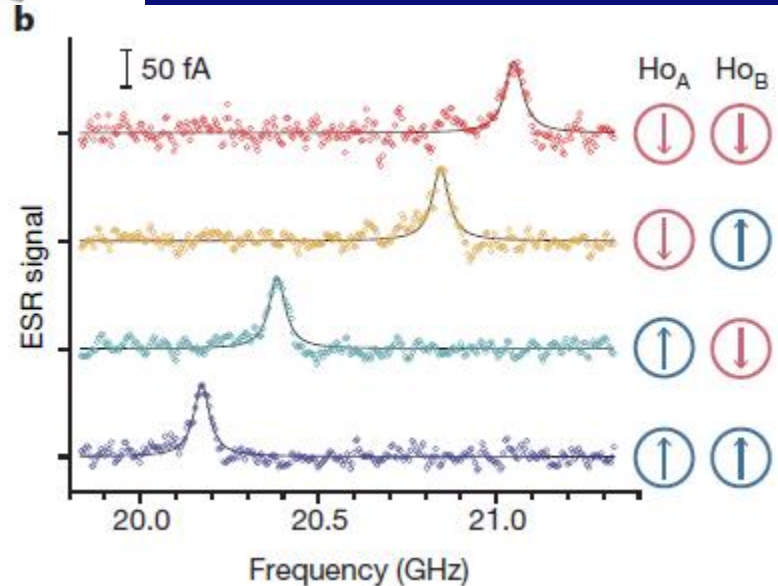
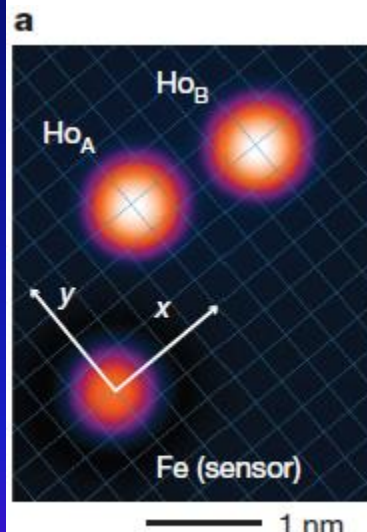
SP-STM with Time Resolution

Single-Atom Dynamics



S. Baumann *et al.*, Science, 417, 350 (2015)

F. D. Natterer *et al.*, Nature, 543, 226 (2017)

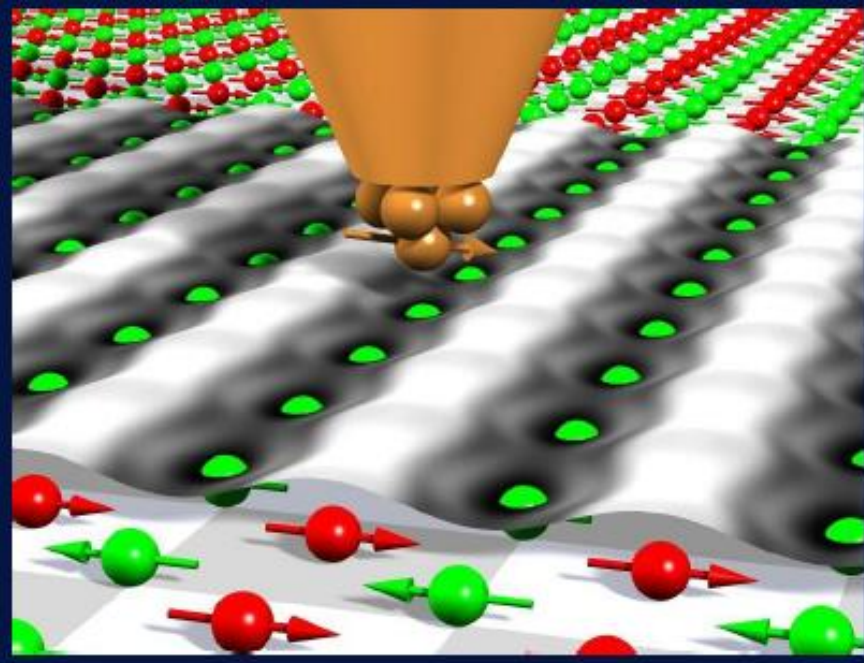


T. Choi *et al.*, Nat. Nanotech., 12, 420 (2017)

Correlation between

- atomic structure
- electronic structure
- spin structure

at ultimate spatial, time
and energy resolution !



Thanks for your attention !